2009

Development and Localization of Spike-Wave Seizures in Animal Models

Damien Jon Ellens
Yale University

Development and Localization of Spike-Wave Seizures in Animal Models

A Thesis Submitted to the

Yale University School of Medicine

in Partial Fulfillment of the Requirements for the

Degree of Doctor of Medicine

by

Damien J. Ellens

2009

Abstract:

Animal models allow for detailed investigation of neuronal function, particularly invasive localization and developmental studies not possible in humans. This thesis will review the technical challenges of simultaneous EEG-fMRI, and epileptogenesis studies in animal models, including issues related to anesthesia, movement, signal artifact, physiology, electrode compatibility, data acquisition, and data analysis, and review recent findings from simultaneous EEG-fMRI studies in epilepsy and other fields.

Original research will be presented on the localization of neuronal networks involved during spike-and-wave seizures in the WAG/Rij rat, a model of human absence epilepsy. Simultaneous EEG-fMRI at 9 Tesla, complimented by parallel electrophysiology, including Multiple Unit Activity (MUA), Local Field Potential (LFP), and Cerebral Blood Flow (CBF) measurements were employed to investigate the functioning of neuronal networks. This work indicates that while BOLD signal increases in the Somaotsensory Cortex and Thalamus during SWD are associated with MUA, LFP, and CBF increases, BOLD signal decreases in the Caudate are associated with CBF decreases and relatively larger increase in LFP and smaller increase in MUA.

Complimenting the localization studies, original research will also be presented on the development of spike-and-wave epilepsy in the C3H/Hej mouse, a model which will allow for more advanced genetic and molecular investigation. This work shows seizure development progressing though immature, transitional, and mature stages.

Table of Contents:

1. Introduction to the use of Simultaneous EEG-fMRI:

Neuroscientists have long sought techniques for investigating the neuronal mechanisms of normal behavior and disease. The uniquely enigmatic nature of the brain and the difficulties inherent to its study limited early physiological investigations of brain function. For example, although able to provide great insight into the localization of brain function, lesion studies are inherently destructive, and thus reveal limited information about brain functioning *in situ*. Techniques for the noninvasive monitoring of brain function were needed. The advent of recording electrical brain activity via electroencephalography (EEG) opened new avenues for the noninvasive study of brain activity (Berger 1929). For many years, neuroimaging lagged behind electrophysiological techniques. However, early studies of cerebral hemodynamic responses showed that brain function could be related to measurements of blood flow. Seizures occurring during neurosurgery have long been known to produce a focal blood flow increase in the cerebral cortex (Horsley 1892; Penfield 1933), and early measurements using intracarotid sensors likewise demonstrated increased cerebral blood flow during seizures (Gibbs, Lennox et al. 1934). Advancements in electrical recording and functional imaging technology in recent decades have now made it possible to noninvasively study the brain at sufficiently high temporal and spatial resolutions to reveal fundamental neuronal processes in great detail.

EEG measures extracellular electrical field potentials generated by populations of cortical neurons, and can capture brain electrical activity with excellent temporal resolution. Although EEG provides high temporal resolution, it is limited in its spatial sampling and cannot completely characterize neuronal activity throughout the entire

brain. The spatial resolution of EEG is not sufficient to reveal the contribution of individual brain regions to neuronal function. The electrical signal recorded in the EEG reflects a spatial summation of the underlying cortical electrical activity, and does not sample subcortical areas; thus EEG with scalp electrodes may not detect deeply originating discharges (Gloor 1985).

Neuroimaging techniques offer a comprehensive spatial sampling of the brain and can look deep into subcortical structures noninvasively. Blood oxygen level dependent (BOLD) functional magnetic resonance imaging (fMRI) is a powerful tool, with excellent spatial resolution, for the noninvasive study of hemodynamic and metabolic changes during brain activity. BOLD-fMRI signals depend on blood oxygenation and cerebral blood flow, the specific implications of which we will discuss, and can therefore provide useful information about neuronal activity (Ogawa, Lee et al. 1990; Ogawa, Menon et al. 1993; Ogawa, Menon et al. 1998).

The advent of fMRI has seen an enormous interest in utilizing the technique to study normal and abnormal brain function in *humans.* Furthermore, s*imultaneous* EEG-fMRI is an ideal method to study the interdependent neuronal, neuroenergetic and hemodynamic changes that occur during brain activity. However, human fMRI studies of pathological brain processes have been limited for several reasons. First, because fMRI techniques are highly sensitive to motion, many human studies are limited to the study of neuronal processes with limited movement, such as the spike-wave seizures associated with absence epilepsy, the interictal (between seizures) period of other epilepsy syndromes, or purely cognitive tasks. Second, human studies are inherently less well

controlled than animal models due to intersubject variability, while in animal models consistent experimental methods and invasive techniques can be used.

Animal models offer the opportunity to fully utilize the power of EEG-fMRI methods to noninvasively record normal and abnormal activity throughout the brain. The ictal (during seizure) activity of multiple seizure types can be investigated using animal models, and these studies are not limited by movement as animals can be studied under anesthetized, paralyzed and ventilated conditions. Variables affecting brain activity can be better controlled in animals, such as the onset and type of seizure, and the induction and type of anesthesia. Furthermore, invasive studies of electrical, hemodynamic, and histological properties can be performed in animals to relate fMRI signals to underlying neuronal activity. Thus, simultaneous EEG-fMRI studies of animal models can provide an important contribution to the understanding of many types of neuronal activity, including epilepsy, sleep, and sensory-motor processing. Additionally, studies of animal models can contribute to our knowledge of fMRI interpretation, thereby informing our understanding of neuroimaging studies in humans, and the neuronal basis of human pathology. Human studies of simultaneous EEG-fMRI including those of epilepsy, sleep, evoked activity, behavior and cognition have recently been reviewed elsewhere (Salek-Haddadi, Merschhemke et al. 2002; Ritter and Villringer 2006). Additionaly, many animal MRI studies are highly relevant for investigating changes in functional and structural anatomy, and exploring physiology (Blumenfeld 2007; Grohn and Pitkanen 2007; Hiremath and Najm 2007).

1.1. **Advantages of EEG-fMRI in animal models**:

Animal models offer a number of distinct advantages, compared to human subjects, in utilizing simultaneous EEG-fMRI to study neuronal function. Animal models allow the investigator to exert greater control over the timing and conditions of neurological events, including seizures, sleep and sensory-motor processing. Animal models also allow for the invasive monitoring and control of anesthesia and physiological parameters that may influence neuronal activity and fMRI signal changes. Small animal models allow for the use of higher magnetic field strengths, as the energy required in maintaining a homogenous magnetic field at a given strength is directly related to its size. Studying the hemodynamic response to neural activity at higher field strengths is desirable as it increases the sensitivity to BOLD contrast mechanisms (Menon, Ogawa et al. 1993; Turner, Jezzard et al. 1993; Yang, Wen et al. 1999). Additionally, the use of paralyzed animals allows for the near elimination of movement artifact, important for all fMRI studies and particularly so for studying events associated with excessive muscle activity, such as partial or generalized motor seizures. Finally, balistocardiogram artifact, a common problem in human fMRI, is comparatively minimal in small animals (Sijbers, Vanrumste et al. 2000).

Animal also provide an excellent model for studying the relationship between neuronal activity and cerebral hemodynamic and metabolic responses. These fundamental relationships can be studied with invasive electrophysiological measurements, and multiple imaging techniques (Logothetis, Pauls et al. 2001; Schwartz and Bonhoeffer 2001; Smith, Blumenfeld et al. 2002; Hyder and Blumenfeld 2004; Nersesyan, Hyder et al. 2004; Shmuel, Augath et al. 2006; Maandag, Coman et al. 2007;

Schridde, Khubchandani et al. 2007). Simultaneous EEG-fMRI investigations can guide tissue studies to specific brain regions of interest, and contribute to elucidating molecular mechanisms related to seizure susceptibility or other disorders. Finally, animal models with genetic variants can be studied with simultaneous EEG-fMRI to examine the neurophysiological changes associated with these genes.

1.2. Limitations and Technical challenges of EEG-fMRI in animal models:

Animal models are constrained by the same limitations inherent to any model system, namely that models are only an approximation of human disease, and need to be interpreted with appropriate caution. There are also several technical challenges to simultaneous EEG-fMRI studies of animals related to their size and the spatial constraints due to using relatively high magnetic fields (Blumenfeld 2007; Mirsattari, Ives et al. 2007).

Although desirable for many investigations, recording simultaneous EEG-fMRI in animals presents a number of challenges. Anesthesia must be carefully considered; as we will discuss many anesthetic agents can alter the cerebral hemodynamic response and may alter the neurophysiological behavior under investigation. Guaranteeing the quality of the MR image can be a formidable challenge, as the imaging signals are sensitive to small amounts of movement, and to magnetic susceptibility differences, especially at air-tissue interfaces, that can introduce unwanted distortions. Animal movement in the scanner must be restricted, either by chemical muscular blockade (curarization) or through habituation to a restraining device. Electrodes must be carefully chosen to avoid

unwanted interactions with magnetic fields and with the tissue (e.g. scalp, subdermal, brain) they contact. Lastly, animal physiology must be carefully monitored during experiments utilizing anesthesia (Mirsattari, Bihari et al. 2005).

Investigations of particular brain processes will present their own unique challenges. Animal studies of epilepsy often encounter additional complications, as seizure activity is prone to alteration by commonly used anesthetic agents, seizures may be difficult to induce in anesthetized animals, and motion artifact can occur during seizures (Blumenfeld 2007).

1.2.1. Anesthesia:

Choosing an appropriate anesthetic agent is crucial in simultaneous EEG-fMRI studies; considerations of the agent's effects on the EEG data, fMRI signal intensity, long-term physiology, and on the neurological event being studied must all be carefully considered. Furthermore, anesthetic agents are known to induce changes in the EEG data (Winters 1976; Sloan 1998; Hudetz 2002), and different experimental designs may be best served by different combinations of anesthetic agents.

Anesthetic agents that are inhaled may be ideal for some designs because of the swiftness with which the depth of anesthesia can be adjusted (Makiranta, Ruohonen et al. 2005; Mirsattari, Ives et al. 2005). However, these agents can alter the hemodynamic response. Isoflurane has been found to greatly diminish the BOLD signal changes seen in the gamma-butyrolactone (GBL) induced spike-and-wave discharge (SWD) rat model (Tenney, Duong et al. 2003). Conversely, the use of both fentanyl and haloperidol does

not block the occurrence of SWDs in two rat genetic models of absence epilepsy (Pinault, Leresche et al. 1998; Nersesyan, Hyder et al. 2004). Furthermore, haloperidol can actually increase the frequency of SWDs (Coenen and Van Luijtelaar 1987; Midzianovskaia, Kuznetsova et al. 2001). Fentanyl in combination with haloperidol has also been used successfully to produce anesthesia without blocking tonic-clonic seizures in a rat model (Nersesyan, Hyder et al. 2004; Schridde, Khubchandani et al. 2007).

A change in the signal strength of the BOLD-fMRI signal compared to the awake state can be seen with anesthetic agents such as alpha-chloralose (Shulman, Rothman et al. 1999; Peeters, Tindemans et al. 2001; Hyder, Rothman et al. 2002; Smith, Blumenfeld et al. 2002) propofol (Katariina M. Lahti 1999) and halothane (Maandag, Coman et al. 2007). In a porcine model sudden deepening of thiopental anesthesia in nonepileptic animals produced significant signal changes in the fMRI response (Makiranta, Jauhiainen et al. 2002). High dose morphine and the sedating antihistamine aceproamzine was found to provide adequate anesthesia in a sheep model of penicillin induced focal epilepsy with minimal EEG suppression (Opdam, Federico et al. 2002). Alpha-chloralose with urethane has been successfully used in a rat model of pentylenetetrazol induced seizures (Keogh, Cordes et al. 2005). Ketamine and xylazine produces adequate anesthesia without blocking limbic seizures studied by fMRI (Englot, Mishra et al. 2008).

In a rat model halothane was found to have no effect on the BOLD response at doses that showed a clear reduction in the baseline neuronal activity on EEG, while a transition from halothane to alpha-chloralose showed an immediate reduction in the spatial extent of the BOLD response without a change in the peak signal change, which evolved over several hours to an increase in both the spatial extent and peak signal

change of the BOLD signal (Austin, Blamire et al. 2005; Maandag, Coman et al. 2007). Halothane has been successfully used to induce temporary anesthesia in rodent models during subject preparation, with data acquired from paralyzed non-anesthetized animals treated with mivacurium (Van Camp, D'Hooge et al. 2003), however, special training is needed for non-anesthetized preparations as discussed shortly. Halothane is commonly used as an induction agent to allow rapid anesthesia of an animal for placement of intravascular lines, tracheostomy, electrodes and placement in a holding apparatus for positioning of the surface coil (Nersesyan, Hyder et al. 2004; Schridde, Khubchandani et al. 2007). A one hour period has been used to allow complete wash-out of the halothane (Keogh, Cordes et al. 2005).

Limiting the use of general anesthesia to the period of preparing the animal with reversal of the anesthesia during simultaneous EEG-fMRI acquisition has also been accomplished with the combination of the anesthetic medetomidine **(**alpha 2 adrenoreceptor agonist) and the reversal agent atipamezole (alpha 2-adrenergic antagonist) in rats (Tenney, Duong et al. 2003), or with ketamine and medetomidine reversed with atipamezole in rats (Tenney, Duong et al. 2004; Brevard, Kulkarni et al. 2006), or with the combination of medetomidine, ketamine and isoflurane reversed with atipamezole in marmoset monkeys (Tenney, Marshall et al. 2004).

In situations where significant movement does not occur, such as during spike-wave seizures, the study of unanesthetized animals may be feasible (Tenney, Duong et al. 2003; Van Camp, D'Hooge et al. 2003). This raises additional technical challenges, as lengthy training of animals is necessary to habituate them to the recording procedures (Khubchandani, Mallick et al. 2003; Sachdev, Champney et al. 2003). Recording from

awake animals can further be facilitated by the use of a topical anesthetic (e.g. lidocaine gel) at any pressure points from restraint devices or needle electrodes (Tenney, Duong et al. 2004; Tenney, Marshall et al. 2004). Performing simultaneous EEG-fMRI studies in awake animals is an important technical challenge to overcome as these studies more closely resemble human studies of conscious subjects.

The anesthetic approaches discussed show great promise in expanding the utility of EEG-fMRI studies in animal models, and in contributing to our understanding of human studies. The wide variety of successful protocols illustrates the importance of tailoring the experimental design to the specific animal model and research question being investigated.

1.2.2. Movement: Curarization and Habituation:

As in human studies, subject movement must be addressed in studies with animal models to limit the creation of artifact in the MR images. As previously discussed, anesthetic agents must be carefully considered for possible interference with the neurological event being studied, and for possibly altering the hemodynamic response. Lightly anesthetized preparations or unanesthetized preparations are advantageous for preserving the normal electrophysiology and neurovascular response but will increase the likelihood of movement by the subject. This has been overcome by curarization with non-depolarizing neuromuscular blockers, such as mivacurium (Van Camp, D'Hooge et al. 2003), pancuronium (Opdam, Federico et al. 2002; Makiranta, Ruohonen et al. 2005), d-tubocurarine (Nersesyan, Hyder et al. 2004; Schridde, Khubchandani et al. 2007;

Englot, Mishra et al. 2008), or vacuronium (Mirsattari, Wang et al. 2006). Curarization requires the animal be ventilated and their physiology monitored throughout the experiment.

Habituation to the restraint device and noise of the MRI scanner is required for the study of awake and conscious animals. This has been accomplished through the use of habituation to a custom designed restraint devices in rats (Khubchandani, Mallick et al. 2003; Sachdev, Champney et al. 2003). Habituation to a restraint device may be facilitated by positive reinforcement (e.g. chocolate milk) combined with diazepam administrated one hour prior to data acquisition to minimize stress (Sachdev, Champney et al. 2003).

It is critical to review data carefully after acquisition for movement artifact using methods such as cine review and center of mass analysis (Nersesyan, Hyder et al. 2004) and to reject data in which significant movement occurs, since even tiny movements can produce large false fMRI signal changes on difference calculations.

1.2.3. Physiology:

Physiological stability is crucial in the study of animals during simultaneous EEG-fMRI. Animal models are commonly studied using inhaled anesthetic agents which require that the animal undergo a tracheostomy and be ventilated. Animals require physiological stabilization for the duration of the experiment (Wood, Klide et al. 2001). Monitoring of heart rate, blood pressure, temperature and ventilation rate can be done continuously (Nersesyan, Hyder et al. 2004; Schridde, Khubchandani et al. 2007).

Arterial blood gas measurements of pH, pCO2, and pO2 can be performed to monitor the physiological state of the animal, as these parameters will affect the hemodynamic response and may affect neuronal function (Jones, Berwick et al. 2005; Mirsattari, Bihari et al. 2005). Mechanical ventilation may be required for some anesthesia regiments or when muscle paralysis is used (Nersesyan, Hyder et al. 2004; Tenney, Duong et al. 2004; Schridde, Khubchandani et al. 2007). Mechanical ventilation, blood pressure monitoring and anesthesia delivery machinery should be kept far from the imaging field to avoid disturbances in the images. This equipment is preferably kept outside of the room containing the magnet, which ideally is itself magnetically shielded.

Hypercapnia can alter the cerebral hemodynamic response, causing vasodilatation of veins and microcapillaries in rat cortex at even mild levels (Nakahata, Kinoshita et al. 2003). Hypercapnia has also been shown to reduce blood flow and volume changes during whisker stimulation, and may also affect changes in the BOLD-fMRI signal (Jones, Berwick et al. 2005). Furthermore, hypercapnia can alter neuronal activity in rats (Kida, Rothman et al. 2007) possibly by inducing periods of cortical desynchronization that may be associated with changes in oxidative metabolism (Martin, Jones et al. 2006).

1.2.4. MRI compatible electrodes:

MRI compatible electrodes and EEG recording equipment has been developed and utilized in multiple studies using simultaneous EEG-fMRI (Mirsattari, Ives et al. 2007). EEG electrodes commonly contain metals that are affected by an external magnetic field; silver-silver chloride (Ag/AgCl), gold-plated silver, platinum, stainless

steel, and tin. Silver and copper electrodes are theoretically compatible with MRI but are not appropriate for invasive recording that may involve direct contact of the electrode to brain tissue due to possible toxicity (Babb and Kupfer 1984). Gold and platinum electrodes have been found to be non-toxic to living tissue (Tallgren, Vanhatalo et al. 2005). Custom-made gold electrodes were found to be superior compared to both custom-made carbon, and commercial platinum-iridium alloy electrodes in size, and effect on image quality (Jupp, Williams et al. 2006). However, gold and platinum may cause artifacts in MR images due to differences between their magnetic susceptibly and that of brain tissue (Mirsattari, Ives et al. 2007). Choosing appropriate MRI compatible EEG recording equipment will depend on whether the goal is for scalp, subdermal, or intracranial recordings.

Scalp and subdermal electrodes have the advantage of leaving the brain intact and theoretically will introduce the least amount of artifact in the MR images. Carbon fiber electrodes are the most widely used material for EEG with simultaneous MRI; for scalp (Van Audekerkea, Peeters et al. 2000) and subdermal recordings (Nersesyan, Hyder et al. 2004; Makiranta, Ruohonen et al. 2005; Schridde, Khubchandani et al. 2007), and directly overlying the cortex via insertion through burr holes (Mirsattari, Wang et al. 2006). Carbon fiber electrodes can also be used for intracranial recordings (Opdam, Federico et al. 2002; Mirsattari, Ives et al. 2005). Teflon coated silver-silver chloride (Ag/AgCl) electrodes can be used alone or in combination with carbon fiber electrodes (Mirsattari, Ives et al. 2005; Young, Ives et al. 2006). fMRI compatible electrodes designed for human use, such as conductive plastic cups and gold plated silver disc

electrodes attached to copper wires can be used in larger animal studies (Mirsattari, Ives et al. 2007).

Intracranial EEG recordings with simultaneous fMRI has the advantage of recording neuronal activity from specific areas of the brain, such as the occipital cortex (Logothetis, Pauls et al. 2001; Shmuel, Augath et al. 2006), or from the site of seizure induction in animal models of focal epilepsy (Opdam, Federico et al. 2002; Englot, Mishra et al. 2008). However, intracranial electrode placement increases the risk of damaging the cerebral cortex and may cause artifact in the MR images if there is bleeding under the burr holes or at the craniotomy site (Mirsattari, Ives et al. 2007). Burr holes should be made with a drill that is compatible with MRI, for example, one coated by titanium or made of diamond to avoid artifacts from any metallic particles the drill may leave (Mirsattari, Ives et al. 2007).

Intracranial electrodes may also be used for stimulating brain regions during fMRI experiments. Electrical stimulation has been accomplished in the rat; including in the motor cortex with carbon fiber electrodes (V.C. Austin 2003), in the amygdale kindling model with custom made carbon and gold electrodes, and commercial platinum-iridium electrodes (Jupp, Williams et al. 2006), in rat medial thalamus with glass-coated carbon fiber microelectrode (Shyu, Lin et al. 2004), and in perforant pathway (Angenstein, Kammerer et al. 2007) and dorsal hippocampus using bipolar tungsten electrodes (Englot, Mishra et al. 2008). Precise electrical stimulation of the Macaque monkey visual cortex using custom glass-coated iridium microelectrodes during fMRI signal acquisition has also been done (Tolias, Sultan et al. 2005).

1.3. fMRI Signal Generation:

The BOLD fMRI signal (S) is only indirectly related to neuronal activity. Animal models provide an excellent opportunity to more precisely investigate this relationship. Neuronal activity consumes energy, which is repleted through increased delivery of oxygen and nutrients via neurovascular coupling. Measurement of S depends on levels of oxygenated hemoglobin (Ogawa, Menon et al. 1998), and therefore on the balance between oxygen delivery and consumption. During neuronal activity, there is an increase in cerebral blood flow (CBF) and oxygen delivery through neurovascular coupling, but there is also an increase in the cerebral metabolic rate of oxygen consumption ($CMRO_2$) (Ogawa, Menon et al. 1998; Hyder, Kida et al. 2001). Increased oxygen delivery normally exceeds oxygen consumption, so that S usually increases in response to increased neuronal activity. However, as we will discuss below, exceptions can occur, especially during the intense neuronal activity accompanying tonic-clonic seizures. The complex relationship between changes in BOLD signal compared to baseline ($\Delta S/S$) and physiology is given in Equation 1. (Kennan, Zhong et al. 1994; Weisskoff, Zuo et al. 1994; Ogawa, Menon et al. 1998).

$$\Delta S/S = Á\ [(\Delta CBF/CBF - \Delta CMRO_2/CMRO_2)/(1+\Delta CBF/CBF) - \Delta CBV/CBV]$$

Equation 1. This equation shows the relationship of the BOLD signal change ($\Delta S/S$) to the changes in the cerebral metabolic rate of oxygen consumption ($\Delta CMRO_2/CMRO_2$),

cerebral flood flow (ΔCBF/CBF), and cerebral blood volume (ΔCBV/CBV). Where Á is a measurable physiologic and magnetic field dependent constant.

Because the majority of neuronal energy is ultimately produced through oxidative metabolism (Shulman, Rothman et al. 2004) measuring changes in the $CMRO_2$ offers the most direct neuroimaging measure of neuronal activity.

1.3.1. Measurement of $CMRO_2$ by MR spectroscopy:

fMRI signals originate in changes in energy consumption and blood flow. Neuronal activity is dependent on neurotransmission, and the stoichiometry of glutamate and GABA neurotransmission, and the energy consumption supplied by glucose oxidation, as has been established in vivo by ^{13}C magnetic resonance spectroscopy (MRS) (Rothman, Sibson et al. 1999). The relationship between neuronal activity and energy consumption provides insight into brain function, and the interpretation of the neuroimaging signal obtained in fMRI experiments (Shulman, Hyder et al. 2001; Shulman, Hyder et al. 2002). Early ^{13}C-MRS experiments in animals and humans used glucose labeled at the C1 carbon atom (Behar, Petroff et al. 1986; Gruetter, Novotny et al. 1994). Infused glucose-C1 enters the TCA cycle via pyruvate dehydrogenase activity and labels glutamate-C4 in the first turn of the neuronal TCA cycle. The C3 and C2 carbon atoms are labeled in the following turn of the cycle. Thus, the time course of ^{13}C turnover of glutamate-C4 can be converted into a measure of the neuronal TCA cycle

flux (Mason, Behar et al. 1992; Mason, Gruetter et al. 1995; Gruetter, Seaquist et al. 1998).

1.3.2. Estimation of $CMRO_2$ by calibrated BOLD:

Equation 1 can be rearranged and approximate $CMRO_2$ maps can be obtained where $\Delta CMRO_2/CMRO_2$ can be calculated by using the data from separate measurements of $\Delta CBF/CBF$, $\Delta S/S$ and $\Delta CBV/CBV$ in the same experiment (Kida, Kennan et al. 2000; Hyder 2004). This technique is referred to as calibrated BOLD, and has been validated by showing good agreement with $CMRO_2$ measurements made using MRS during somatosensory stimulation over a wide range of conditions (Hyder, Kida et al. 2002). Changes in spiking frequency have been directly linked to calibrated fMRI measurements of energetics in rat somatosensory cortex (Smith, Blumenfeld et al. 2002). Calibrated BOLD allows $CMRO_2$ maps to be obtained at the same spatial and temporal resolution as fMRI, which is much higher than in MRS experiments. Although $CMRO_2$ can be measured by neuroimaging methods, the BOLD-fMRI signal is a more convenient, although indirect, method of mapping neuronal activity.

1.3.3. CBV:

The relative changes in CBV from baseline can be measured by the administration of a high susceptibility MRI contrast agent to enhance the blood volume induced changes (Hyder, Kida et al. 2002). AMI-227, an ultrasmall iron oxide colloid contrast agent can

be used, and remains in the intravascular space for several hours (Kennan, Zhong et al. 1994).

1.3.4. CBF:

Absolute CBF maps can be obtained by using spin-echo slice selective and non-slice selective inversion-recovery weighted EPI data (Hyder, Kida et al. 2001). Arterial spin labeling (ASL) MRI utilizes endogenous water as a magnetic contrast agent. Blood water flowing to the brain is saturated in the neck region with a slice-selective saturation imaging sequence, creating an endogenous tracer in the form of proximally saturated spins. This technique allows regional perfusion maps to be measured noninvasively (Detre, Leigh et al. 1992; Detre and Wang 2002). Optical imaging techniques like laser Doppler flowmetry (LDF) can measure CBF, although these methods differ in the underlying physical mechanisms from ASL-MRI (He, Devonshire et al. 2007). LDF values for CBF have proven useful in calculating $CMRO_2$ and are comparable to CBF measurements acquired using ASL-MRI (Mandeville, Marota et al. 1999; He, Devonshire et al. 2007; Schridde, Khubchandani et al. 2007).

1.4. Signal Artifact and Artifact removal:

Signal artifact presents an additional problem as fMRI equipment can cause artifact in the EEG recording in general, and particularly during image acquisition (Ives, Warach et al. 1993) and EEG equipment can cause significant artifact in the fMRI images

(Krakow, Allen et al. 2000). Gradient coil induced magnetic field variations and radiofrequency pulses associated with image acquisition can cause high voltages in the EEG recording electrodes that obscure EEG signals. Revealing the full EEG signal may require removal of the MRI artifact through offline digital filtering, including simple low-pass frequency filtering (Nersesyan, Hyder et al. 2004), or using methods such as temporal principle component analysis (Negishi, Abildgaard et al. 2004). Care must be taken in placing the EEG electrodes on the animal skull in such a way as to minimize unwanted magnetic field inhomogeneity and image distortion (Nersesyan, Hyder et al. 2004).

Movement-related artifact has already been discussed, and any runs containing significant movement should be rejected from the analysis. Low frequency drift can also occur, especially during prolonged fMRI acquisitions, which may be related to a number of physiological or technical factors. It is important to be aware of these slow signals, and to take them into consideration when planning data analysis, or to prevent them at the source when appropriate. Although low frequency drift in some situations can be related to physiology, in other cases it can be shown to occur due to purely technical factors and not physiology (e.g. by demonstrating similar drift when scanning a phantom, or a non-living perfused brain).

1.5. Data analysis:

Data analysis of simultaneous EEG-fMRI experiments allows for pairing of fMRI acquisitions with neuronal signal. Prior knowledge of the time course of CBF changes

during the neuronal function being studied will direct the analysis of the fMRI signal. For example, in analyzing fMRI signals during rodent spike-wave discharges (SWD) prior measurements using LDF showed that CBF peaked 3 to 4 seconds after SWD onset began on EEG, and then decreased back to baseline after 3 to 4 seconds (Nersesyan, Herman et al. 2004). Pixel based measurements of the BOLD signal response showed a similar time course (Nersesyan, Hyder et al. 2004). Therefore, in constructing functional maps of BOLD signal changes during SWD compared to baseline it was first assumed that each BOLD image acquisition should be related mainly to SWD occurring in the preceding 5 second EEG interval. Pairs of consecutive images and associated pairs of consecutive EEG intervals were selected where the first EEG interval contained quiet EEG baseline, and the second contained SWD (Nersesyan, Hyder et al. 2004). t-maps were then constructed by contrasting the set of baseline images to SWD images on a pixel-by-pixel basis (Nersesyan, Hyder et al. 2004). t-maps can also be constructed by be combined with region of interest (ROI) analysis to evaluate differences in BOLD signal change and time course limited to specific brain regions (Tenney, Duong et al. 2003; Tenney, Duong et al. 2004; Tenney, Marshall et al. 2004; Schridde, Khubchandani et al. 2007).

The time course of generalized tonic-clonic seizures (GTCS) begins with an abrupt onset of sustained, high-frequency neuronal firing during the tonic phase, followed by rhythmic high-frequency firing in the clonic phase (Matsumoto and Marsan 1964; Avoli, Gloor et al. 1990), with a total duration of several minutes. Therefore, analysis of more prolonged events such as tonic-clonic seizures requires a different approach to analysis. Comparison of bicuculline induced tonic-clonic seizures to baseline activity has

been done by comparing a set of baseline images before bicuculline injection to a set of images after seizure onset (Nersesyan, Hyder et al. 2004; Schridde, Khubchandani et al. 2007). t-maps can then be constructed by comparing the set of baseline images to the set of images during the beginning of seizure activity (Nersesyan, Hyder et al. 2004; Schridde, Khubchandani et al. 2007).

Hierarchical clustering algorithms can also be used to identify voxels of interest in the fMRI data (Keogh, Cordes et al. 2005). The clustering analysis utilizes a t-test applied independently to each voxel, comparing a chosen baseline period to a period of signal activity; voxels without significant changes are discarded. Voxels that are acting similarly to another portion of brain can be chosen by applying a further test requiring that each voxel have a correlation with two other voxels. This has been applied in the study of pentylenetetrazol (PTZ) induced seizures in rats (Keogh, Cordes et al. 2005).

Changes in $CMRO_2$ can be estimated for individual brain regions using the known general relationship between oxygen consumption and BOLD, CBV, and CBF data at steady state (Equation 1) (Kida, Rothman et al. 2007; Schridde, Khubchandani et al. 2007). This can be done using CBF values obtained from ASL-MRI or from LDF, together with separate measurements of BOLD and CBV (Schridde, Khubchandani et al. 2007).

1.6. Sequential EEG-fMRI Studies in Animals:

Experimental designs where the timing of the hemodynamic response is relatively controlled may circumvent the technical challenges inherent to simultaneous EEG-fMRI

studies by using *sequential* EEG-fMRI. These studies record the EEG-fMRI under the same conditions and where the time course is relatively consistent allowing for investigation of both neuronal electrical data and cerebral hemodynamic responses. Sequential EEG-fMRI has been employed to study epilepsy in the rat model of pentylenetetrazol induced seizures (Keogh, Cordes et al. 2005; Brevard, Kulkarni et al. 2006). Sequential electrical recording and BOLD-fMRI has also been used to investigate visual processing in the cat (Kayser, Kim et al. 2004).

Sequential investigations are limited in the accuracy with which fMRI signals can be correlated to EEG activity. Therefore, sequential measurements are not ideal for the study of animal models where the neuronal function under investigation is variable, and where the variability is an important aspect of the phenomenon being studied.

1.7. Simultaneous EEG-fMRI in Animals:

Simultaneous EEG-fMRI investigations of animal models have distinct advantages, as previously mentioned, in the correlating of brain electrical, hemodynamic and neurometabolic responses. Simultaneous EEG recording with MRI was first performed in a rat cortical spreading depression model in 1995 (Busch, Hoehn-Berlage et al. 1995). Subsequent EEG-fMRI studies in animal models have mainly focused on epilepsy. Here, we will review EEG-fMRI animal studies of epilepsy, including generalized and partial seizures, sleep, and studies where electrical stimulation was applied during signal acquisition. We will also discuss animal studies where the primary

aim was to investigate the relationship between neuronal activity and the BOLD signal response.

1.7.1. Epilepsy:

The first animal model studies of epilepsy with simultaneous EEG-fMRI were performed less than a decade ago (Van Audekerkea, Peeters et al. 2000). As we have mentioned, animal models allow the full power of fMRI methods to be employed to noninvasively map epileptic activity throughout the brain. Animal models provide a means study the ictal activity of all seizure types, and are not limited by movement artifact as animals can be studied under anesthetized, paralyzed and ventilated conditions. The onset and type of seizure can be controlled in animal models, and invasive studies can be done to relate fMRI signals to underlying neuronal activity (Blumenfeld 2007).

Simultaneous EEG-fMRI in epilepsy can be used to accomplish several goals, including the accurate localization of seizure onset, the evolving physiology of seizures in focal regions or distributed networks, and to relate fMRI signals to underlying physiology. Interpretation of human studies will be improved by a better understanding of the relationship between neuronal activity and the fMRI signal in animal models. A better understanding of the local networks and brain regions involved in specific seizure disorders may help design improved focal resective surgery, and could provide targets for deep brain stimulation, medication or even gene therapy. Animal studies may also improve our understanding of functional brain impairment and cognitive dysfunction (Blumenfeld and Taylor 2003; Blumenfeld 2005).

1.7.1.1. Absence Seizure Models:

Human studies of spike-wave discharges (SWD) in absence epilepsy patients (Archer, Abbott et al. 2003; Salek-Haddadi, Lemieux et al. 2003; Aghakhani, Bagshaw et al. 2004) have revealed a great deal regarding the neural networks involved in SWD formation and propagation. However, additional information is needed to correctly interpret fMRI signal increases and decreases in this disorder. Animal models can be used to study in depth the relationship of fMRI signal changes to underlying neuronal activity, and molecular mechanisms during SWDs (Blumenfeld 2005). The Wistar AlbinoGlaxo rats of Rijswijk (WAG/Rij) have spontaneous spike-and-wave discharges, and are an established model of human absence epilepsy (Coenen and Van Luijtelaar 2003). fMRI studies in this model have shown BOLD signal increases in focal bilateral regions of the cortex and thalamus (Nersesyan, Hyder et al. 2004). Interestingly, although considered a generalized seizure disorder, focal anterior regions of the brain are most intensely involved both in fMRI and electrical recordings of SWD, while other brain regions are relatively spared (Meeren, Pijn et al. 2002; Nersesyan, Hyder et al. 2004). Although human fMRI studies of SWD have shown both increase and decreases in the cortex (Archer, Abbott et al. 2003; Salek-Haddadi, Lemieux et al. 2003; Gotman, Grova et al. 2005; Labate, Briellmann et al. 2005; Aghakhani, Kobayashi et al. 2006; Hamandi, Salek-Haddadi et al. 2006; Laufs, Lengler et al. 2006), studies in WAG/Rij rats have so far shown mainly increases in the cortex (Nersesyan, Hyder et al. 2004; Tenney, Duong et al. 2004). However, recent studies have shown that the basal ganglia show

prominent fMRI signal decreases during SWD in rodent models (Guillemain, David et al. 2007; Mishra, Schridde et al. 2007).

Gamma-butyrolactone (GBL) is a precursor of gamma-hydroxybutyrate, and produces robust SWD in rats, resembling petit mal status epilepticus (Snead, Depaulis et al. 1999; Tenney, Duong et al. 2003). A simultaneous EEG-fMRI study, using epidural electrodes, of SWD in rats treated with GBL showed thalamic increases and mixed cortical increases and decreases in fMRI signals (Tenney, Duong et al. 2003). However, a similar study in marmoset monkeys given GBL showed only fMRI increases during SWD (Tenney, Marshall et al. 2004).

1.7.1.2. Generalized Tonic-Clonic Seizure Models:

Generalized tonic-clonic seizures (GTCS) in animal models can be induced by pharmacologic means, allowing the researcher control over the timing of seizures. The first investigation of GTCS using fMRI was performed over 15 years ago (Ogawa and Lee 1992). Simultaneous EEG-fMRI studies of GTCS in animals face the challenge of constraining movement in the scanner (Van Camp, D'Hooge et al. 2003; Nersesyan, Hyder et al. 2004; Schridde, Khubchandani et al. 2007).

Kainic acid, a potent central nervous system stimulant, has been used to induce GTCS in animals (Ben-Ari, Lagowska et al. 1979). A distinct change in the BOLD-fMRI signal has been seen following injection of kainic acid (Ogawa and Lee 1992). Another proconvulsive agent, pentylenetetrazol, an antagonist of GABA, has also been used to induce GTCS in rats (Van Camp, D'Hooge et al. 2003; Keogh, Cordes et al. 2005;

Brevard, Kulkarni et al. 2006). Finally, bicuculline, another GABA receptor antagonist, has also been used to induce rat GTCSs, showing widespread cortical BOLD-fMRI increases (Nersesyan, Hyder et al. 2004; Schridde, Khubchandani et al. 2007).

Studies of bicuculline induced GTCS using multiple techniques to investigate neuronal activity, CBF, CBV, $CMRO_2$, and BOLD signal changes, indicate that these parameters all increase in parallel in the cortex during bicuculline-induced GTCS. In contrast, some regions such as the hippocampus may show variable BOLD signal changes or even BOLD decreases even though direct recordings of neuronal activity from the hippocampus showed consistent large increases in neuronal activity during GTCS (Schridde, Khubchandani et al. 2007). Interestingly, the CBF increase exceeded the $CMRO_2$ increase in the cortex, producing the expected consistent increase in BOLD. However, in the hippocampus, CBF increases did not on average exceed $CMRO_2$ so that mismatch between metabolism and CBF can lead to paradoxical BOLD decreases in some cases (Schridde, Khubchandani et al. 2007).

1.7.1.3. Partial Seizure Models:

Simultaneous EEG-fMRI in animal models of focal epilepsy necessitates additional operative techniques to induce localized seizure activity. Where genetic and systemic pharmacologic models allow the study of generalized seizure disorders, direct focal introduction of seizure inducing drugs, commonly penicillin, or electrical stimulation is required to cause focal seizures. One such early study used focal penicillin infusion into the prefrontal cortex of sheep (Opdam, Federico et al. 2002). Localized

increases in the fMRI signal were identified in the sheep cortex during seizures (Opdam, Federico et al. 2002). Penicillin has also been applied to the somatosensory cortex in a porcine model, showing regional signal increases during interictal spikes (Makiranta, Ruohonen et al. 2005), and to the occipital cortex in rats, showing regional signal increases during seizures (Mirsattari, Wang et al. 2006).

Electrical stimulation of the hippocampus has been recently been performed during simultaneous depth electrode and fMRI (Englot, Mishra et al. 2008). Following electrical stimulation, neuronal electrical activity increased intensely in the hippocampus. BOLD signal increases were also observed in the hippocampus, as well as in the thalamus and septal nuclei during seizures. Separate experiments also showed neuronal electrical activity increases in the thalamus and septal nuclei in this model. In addition, BOLD decreases were seen in the orbital frontal cortex (Englot, Mishra et al. 2008) which may resemble decreases in neocortical function seen during human limbic seizures (Blumenfeld, McNally et al. 2004; Blumenfeld, Rivera et al. 2004).

1.7.2. Sleep:

Simultaneous EEG-fMRI has also been used to investigate sleep in rodent models (Khubchandani, Jagannathan et al. 2005). Simultaneous EEG allows for the determination of sleep and wake cycles in the animal while scanning. fMRI signal increases were shown in the medial preoptic area during sleep, corroborating other work indicating the importance of this area in maintaining slow wave sleep (Khubchandani,

Jagannathan et al. 2005). Simultaneous EEG-fMRI has been used primarily in epilepsy research, but potential exists for much additional work in other fields, including sleep.

1.7.3. Sensory-motor stimulation models:

Simultaneous EEG-fMRI can be used to study activation of specific brain regions during sensory-motor stimulation. Electrical forepaw stimulation has been used to compare cortex activation during fully conscious curarization compared to during alpha-chloralose anesthesia (Peeters, Tindemans et al. 2001). Simultaneous acquired EEG data was used to identify the awake and anesthetized states, showing that the BOLD signal was smaller under alpha-chloralose anesthesia, compared to the awake state (Peeters, Tindemans et al. 2001). Simultaneous EEG-fMRI has also been used to study the interaction between simultaneous and sequential electrical forepaw stimulations in the rat and the effects on the associated stimulation evoked potentials and BOLD signal responses (Ogawa, Lee et al. 2000) showing fMRI signal modification in response to two stimuli directly following another, although on EEG the changes associate with the second stimulation was extinguished.

Studies investigating fMRI changes during anesthesia with parallel electrophysiology recordings during forepaw stimulation are ongoing, and have recently shown differences in the strength of fMRI changes under different types of anesthesia (Hyder, Rothman et al. 2002; Smith, Blumenfeld et al. 2002; Maandag, Coman et al. 2007).

1.8. Relating fMRI Signals to Electrophysiological Recordings:

One of the major goals of animal studies in this field is to relate neuroimaging signals to underlying electrical neuronal activity. Direct measurement of neuronal activity in these models is therefore essential. Simultaneous recordings of single neurons, local field potential (LFP) and BOLD fMRI signals has been accomplished in anesthetized monkeys (Logothetis, Pauls et al. 2001; Tolias, Sultan et al. 2005; Shmuel, Augath et al. 2006), but this method remains a significant challenge technically.

The relationship between fMRI signals and electrophysiology can be successfully investigated by parallel benchtop electrophysiology and fMRI experiments performed under identical conditions (Hyder, Kida et al. 2002; Smith, Blumenfeld et al. 2002). Studies designed to investigate both modalities in the same animal model have shown good correspondence between fMRI increases and physiological measurements (Nersesyan, Herman et al. 2004; Schridde, Khubchandani et al. 2007). Specifically, anterior brain regions such as the somatosensory cortex where fMRI signals are increased during SWD show increased neuronal firing and CBF, while posterior areas such as visual cortex spared by fMRI signal changes show few changes in physiological measurements (Nersesyan, Hyder et al. 2004). Direct physiologic measurements during generalized tonic-clonic seizures, on the other hand, show increases in both anterior and posterior brain regions, in agreement with fMRI measurements in the same areas (Nersesyan, Hyder et al. 2004). Interestingly, in the somatosensory cortex, the magnitude of BOLD fMRI, neuronal firing, and CBF changes were greatest for generalized tonic-clonic seizures, less for normal whisker stimulation, and even less for SWD (Nersesyan,

Herman et al. 2004; Nersesyan, Hyder et al. 2004). Understanding the relationship between fMRI signal increases and decreases in other regions will be the subject of future investigations, as will understanding the neuroenergetic mechanisms of fMRI signal changes.

2.1 Introduction to localization in WAG/Rij rat and development in C3H/Hej mouse:

Multi-modal fMRI experiments including BOLD, CBF, and CBV imaging, with simultaneous EEG recordings were performed in Wistar albino Glaxo rats of Rijswijk (WAG/Rij), an established animal model of human absence epilepsy (Coenen, Drinkenburg et al. 1992; Meeren, Pijn et al. 2002). WAG/Rij rats exhibit spontaneous episodes of staring and unresponsiveness accompanied by SWD, which resembles human absence seizures in behavior, electroencephalography and anit-epileptic drug sensitivity (Coenen and Van Luijtelaar 1987; Peeters, Spooren et al. 1988; van Rijn, Sun et al. 2004). We also performed parallel invasive electrophysiology and cerebral blood flow analysis on WAG/Rij rats to directly measure neuronal firing rates, local field potential, and blood flow changes in regions of interest during SWD. This approach made possible the calculation of the cerebral metabolic rate of oxygen consumption and allowed hemodynamic response functions to be calculated for individual regions of interest. The methodology for functional imaging and electrophysiology is complex, but with knowledge and experience rats can be utilized to these type of experiments with success. The benefits of rats, as compared to mice, is their greater size and the greater experience

(as outlined above) of the neuroscience community in using rats for this work. Mice, on the other hand, are difficult to utilize (currently) for imaging studies, however mice are more suitable for investigations into the development of epilepsy on the molecular and genetic level. Although the development of SWD has been characterized in Wistar Albino Glaxo rats from Rijswijk (WAG/Rij)(Coenen and Van Luijtelaar 1987) and in genetic absence epilepsy rats of Strasbourg (GAERS) (Vergnes, Marescaux et al. 1986), rat models are limited by their relative paucity of genetic characterization compared to mouse models In addition, particularly in WAG/Rij rats, onset of SWD takes several months, which can make investigation of epileptogenesis a slow process.

Among mouse models for SWD, (Fletcher, Lutz et al. 1996; Cox, Lutz et al. 1997; Letts, Felix et al. 1998), the C3H/HeJ mouse (Frankel, Beyer et al. 2005) has the advantage of relatively pure absence phenotype (brief episodes of SWD accompanied by behavioral immobility), without other kinds of seizures or neurological impairment such as cerebellar ataxia. A specific genetic defect, namely a mutation of the AMPA receptor subunit *Gria4*, was recently identified as the cause of SWD in C3H/HeJ mice (Beyer, Deleuze et al. 2008). In the interest of furthering progress in our understanding of epileptogenesis and its prevention, we sought to characterize the critical developmental period for SWD development in the C3H/HeJ mouse through serial EEG recordings.

2.2. Methods:

WAG/Rij Rat Animal preparation

All experimental procedures were in full compliance with approved institutional animal care and use protocols. A total of 98 (43 BOLD, 45 electophysiology, 10 CBV) experiments were performed in 41 adult (34 female and 7 male) Wistar albino Glaxo rats of Rijswijk (WAG/Rij) (Harlan, Indianapolis, Indiana, USA) aged (6-16 months) 10 ± 1 months (mean ± SEM) with an average weight of 220 ± 1 g (mean ± SEM) were used in these experiments. 21 animals were used for acute electrophysiological and laser Doppler flowmetry cerebral blood flow recordings. Neurophysiology experiments were included only where electrophysiology recordings captured seizures simultaneously in both regions of interest (recordings were done in CPu, S1BF, and VPM).

C3H/Hej Mice Preparation

All procedures were in full compliance with approved institutional animal care and use protocols. We used a total of 44 C3H/HeJ mice (strain #000659, The Jackson Laboratory, Bar Harbor, Maine, USA,) for all experiments. Mice were housed according to institutional guidelines with free access to food and water on a 12 hour light/dark cycle (lights on at 7am).

Surgical implants and recordings were performed using methods similar to those we used previously (Klein, Khera et al. 2004; Blumenfeld, Klein et al. 2008). Briefly, under ketamine (30mg/kg), xylazine (6mg/kg), and acepromazine (1mg/kg) anesthesia, we implanted tripolar electrodes (Part # MS333/3-A, Tripolar electrode uncut untwisted 0.005; Plastics One Inc., Roanoke, VA; Internal control # 8LMS3333XXXE, Pedestal Height: 8 mm.) using a stereotactic frame (David Kopf Instruments, Tujunga, CA) in mice ranging in age from 5 d to 60 d. To provide good electrical contact, the ends of the

recording electrodes were prepared before wrapping around skull screws by scraping off the polyimide insulation and exposing stainless steel wire up to 10 mm from the tip, leaving insulation intact proximally as verified under the microscope. Level of anesthesia was monitored by respiration, heart rate, glabrous skin perfusion, and response to foot pinch. To anesthetize mice at 5-6 d old, mice were placed on cold packs (Phifer and Terry 1986; Danneman and Mandrell 1997), and physiology and level of anesthesia was monitored as described above. In all animals, small burr holes (using Micro Drill Steel Burrs, 2.3mm shaft diameter, 44mm overall length; Item # 19008-09, Fine Science Tools (USA), Inc.) were made in the skull without disturbing the dura. In mice over ten days old electrodes were secured to the skull using stainless steel screws (Small Parts, Inc., Part # MX-000120-01B-10, binding screw, with shaft length=1/16", size=000, thread=120). For mice less than 10 days of age electrodes were secured with a smaller screw (Small Parts, Inc., Part # MX-0000160-01FL-10, fillister screw, with shaft length=1/16", size=0000, thread=160). EEG recording electrodes were placed at frontal cortex (AP +2.0, ML +2.0 mm from bregma in adult mice, AP +1.0 to +2.0, ML +1.0 to +2.0 from bregma in younger animals), and parietal cortex (AP -6.0, ML +2.0 mm from bregma in adult mice, AP – 4.0 to - 6.0, ML + 1.0 to +2.0 from bregma in younger animals) and a ground electrode was placed in the midline over the cerebellum. Dental acrylic (Cat # 1255710; Henry Schein Inc, Indianapolis, IN; Lang Jet Denture Repair Acylic) was used to fix the electrode pedestal in place. Pups that had not yet been weaned *(pups were typically weaned at 21 days)* were implanted and returned to the dam's cages by implanting the whole litter at the same time, with care taken to fully clean blood and debris from the implantation site. Pups and dams were observed to resume normal

feeding and nesting patterns. Mice were given a post-operative analgesic of carprofen (5 mg/kg subcutaneous immediately and in drinking water for 48 h after surgery) and given a recovery period of at least 24 hours after surgery. EEG signals were recorded via commutator (Plastics One, Inc.) using a Grass CP 511 amplifier (Grass-Telefactor, Astro Med, Inc., West Warwick, RI). Band pass frequency filter settings were 1-300 Hz. Signals were digitized at a sampling rate of 1 kHz with an NI USB-6008 A/D converter and LabView 7.1 software (National Instruments, Austin, TX), and analyzed using Spike 2 (Cambridge Electronic Design, Cambridge, UK). Continuous EEG data were recorded from awake-behaving mice starting at 12:00pm and usually concluding before 6:00pm. Most of the recordings were obtained from each mouse for 3 h per day. Pups that were not yet weaned were removed from their mother's cages just before recording sessions and returned promptly after recording. EEG recording were obtained at the following time points: 5-7d (n=9), 10-15d (n=6), 20-22d (n=8), 23-25d (n=5), 26-30d (n=7), 31-40d (n=11), 41-50d (n=5), and 51-62d (n=9).

WAG/Rij Rat Electrophysiology Recording Parameters

Electrophysiological recordings were acquired over 20-30 minutes under anesthesia. Before electrophysiology experiments, animals were anesthetized with fentanyl (40 μg/Kg, IV) and haloperidol (1 mg/kg, IP). A high-impedance (2-4 MΩ) microelectrode (FHC, Bowdoinham, ME, part #UEWMGGSEDNNM) was placed in two of the following three brain region at a time: caudate-putamen (AP 0.00 and ML +4.0), somatosensory cortex (AP -2.3 and ML -5.02 places at 30^0), and vetral-posterior-medial (VPM) nucleus of the thalamus (AP -3.3 and ML 3.2). Twenty-two experiments (n=13

animals) were performed to record electrical activity and in twenty-three experiments (n=11 animals), an OxyFlo XP needle probe (Oxford Optronix, Oxford, UK, part #MNP110XP-3/50) was fixed to the recording micro electrode to measure CBF along with MUA and LFP. Seven of twenty-three experiments (from 3 rats) recorded for CBF were also used for electrophysiology recordings. 4 seconds of whisker stimulations was done during electrophysiological recordings to verify brain regions. At the end of experiments, animals were euthanized with an IP injection of Euthasol (Virbac AH, Inc., Fort Worth, TX) and brains were collected for histological verification of electrode locations.

A Microelectrode AC Amplifier (Model #1800, A-M Systems, Carlsborg, WA) with broad-band filtered from 0.1 Hz to 10 kHz (×100 gain) was used to record electrical signal during spontaneous spike-wave seizures in WAG/Rij rats under fentanyl and haloperidol anesthesia. Signals were recorded either from S1BF and CPu or from S1BF and VPM simultaneously. Signals were then filtered with a Model #3363 Filter (Krohn-Hite Corporation, Brockton, MA) into LFP (1-100 Hz) and multiunit activity (MUA) (400 Hz - 10 kHz). For CBF measurement experiments, we used a Model # 4000 LDF system (Oxford Optronix, Oxford, UK). Electrophysiology and CBF signals were digitized with a Power 1401 (CED) at a sampling rate of 1 kHz for LFP and CBF and 20 kHz for MUA, and recorded using Spike 2 software.

WAG/Rij Rat fMRI-EEG Data analysis and statistics

EEG signals acquired during MRI experiments were first processed by applying a principal component analysis (PCA) based algorithm (Negishi, Abildgaard et al. 2004) to

reduce residual magnetic field gradient induced artifacts in the EEG recordings. All EEG data were marked for individual SWD onset and offset time in spike 2 software manually using script provided by CED. These marking of SWD onset and offset were used for analyzing time course of BOLD, CBV, electrophysiology, and CBF changes in different brain regions. SWDs were defined as large-amplitude (>2X the background EEG peak-to-peak amplitude) rhythmic 7–8 Hz discharges with typical spike-wave morphology lasting >1.0 second. fMRI images were processed using in-house program running on a MATLAB platform (The MathWorks, Inc., Natick, MA). Although rats were paralyzed during experiments, all fMRI series were first screened for movement artifacts using a MOVIE function and center of mass analysis, restricted to voxels within the brain boundaries, to ensure that all runs exhibited movement of less than 20% of a pixel in either X or Y plane of the center of mass image. For BOLD and flow-related CBV experiments, t-maps were calculated for baseline and activated image acquired after SWD. The t-maps were thresholded for $P < 0.05$ ($t = 2$) to help control for multiple comparisons, and t-map images were superimposed onto corresponding high-resolution anatomical images for each slice and from each individual animal.

WAG/Rij Rat Electrophysiology and CBF experiments

Data were prepared for analysis by defining 1) Baseline images (B) as those within the last 2 seconds of recording before the SWD onset; 2) SWD images (A) as large-amplitude (>2X the background EEG peak-to-peak amplitude) rhythmic 7–8 Hz discharges with typical spike-wave morphology lasting >1.0 s (van Luijtelaar and Coenen 1986). LFP and MUA signal power were processed using Spike 2 software, to see

changes in neuronal activity during recordings of spike-wave seizures (SWD) in anesthetized animals. SWD onset and offset were marked in spike 2 software manually using script provided by CED. These onset/offset (s) marking were used for analyzing time course of electrophysiology and CBF changes. To show time course of mean percent changes in LFP and MUA power during SWD, the root mean square (RMS) voltage was measured in 0.5 s time bins from 2 s before SWD onset (as baseline) to 9 s after SWD onset. Mean LDF signals were also binned in 0.5 s bin to show time course of mean percent change in CBF signals. Data time points were synchronized to the time of SWD onset, and plotted as mean percent change ± standard error of the mean (SEM) from a 2 s uninterrupted baseline recording immediately before SWD onset. We used MUA power as an estimate of action potential firing because this has been shown to correspond well to spiking rate measured by template matching (Shmuel, Augath et al. 2006).

For analysis and comparison of temporal relationship between BOLD and CBV signal changes measured in the caudate-putamen, somatosensory cortex, and VPM, and CBF signal changes recorded in those regions during electrophysiology experiments, regions of interest (ROIs) were chosen for the MRI data analysis based on coordinates (Paxinos and Watson 1998) for the above mentioned brain regions. In addition to the above three ROIs, five additional brain regions were also analysed using ROIs approach to see for BOLD signal timecourse changes. These include the anterior cingulate cortex, retrosplenial/posterior cingulate cortex, hippocampus, superior colliculli, and visual cortex.

SWD onset with respect to fMRI image acquisition start time is variable and thus we arranged SWD events on EEG in each second (i.e. images acquired with start of

SWD, images acquired after 1 s of SWD onset, images acquired after 2 s of SWD onset, and so on) to calculate BOLD signal change time-courses. To determine if signal changes were significantly different between baseline and seizure recordings for all ROIs, the mean percent signal change for 0 to 3.0 s after SWD onset compared to the mean percent signal change during an uninterrupted 2 s baseline immediately before SWD onset were calculated. Paired *t*-tests were used to analyze signal changes during seizures compared with baseline recordings, with significance assessed at $p \leq 0.05$. All graphs are plotted as mean ± SEM over the time range of the experiments in 0.5 s bins and synchronized to time of SWD onset.

Analysis of C3H/Hej Mice EEG data

SWDs were defined as large-amplitude (>2× the background EEG peak-to-peak amplitude) rhythmic 5-8 Hz discharges with spike-wave morphology lasting >1.0 s. We were more liberal in defining spike-wave morphology for the purposes of this study than in prior criteria (Coenen and Van Luijtelaar 1987) so that any precursors of spike-wave activity could be identified at an early age. Intervals containing artifact or slow wave sleep were excluded from the analysis. Start and end time for all SWDs were manually marked and the number of seizures, and seizure durations were then calculated. Percent time in SWD was determined as (sum of SWD interval durations/total usable recording time) × 100%.

Power spectral analysis was performed for mice age 5-7 d (n = 9), 20-22 d (n = 8), and 51-62 (n = 9) on all marked SWD intervals included in the above analysis. Power spectra were calculated for using Spike2 software, with scripts provided by Cambridge

Electronic Design (Cambridge, U.K.). Bin size for the fast Fourier transform was 1.024 s.

2.3. Results:

Ictal BOLD signal changes in spike-wave seizures in WAG/Rij Rats

BOLD fMRI detected both increases and decreases in multiple cortical and subcortical regions from 43 experiments on 20 animals. We found fMRI increases in face somatosensory cortex (S1BF) (43/43 experiments), thalamus (37/43), anterior and posterior cingulate (29/43), and superior colliculi (12/23), and fMRI decreases in the caudate-putamen (28/43) with no change in visual cortex (V1M) (Fig. 1).

CBV signal changes in spike-wave seizures in WAG/Rij Rat

Flow related CBV during SWD were measured during the same experimental session following injection of iron oxide contrast agent (Combidex [ferumoxtran-10], Advanced Magnetics Inc.). CBV measurements demonstrated regional changes which closely resembled BOLD fMRI maps, with CBV increases in the bilateral somatosensory cortex (10/10 experiments) and thalamus (8/10), and decreases in the caudate-putamen (6/10) from 3 animals (Fig. 2).

Neuronal activity and CBF during SWD in WAG/Rij Rats

Electrical recording studies of SWD were performed with extracellular multiunit electrode recordings in 21 WAG/Rij rats, we found that multiunit activity and local field

potentials were maximal in the somatosensory cortex and the thalamic ventral posterior medial nucleus.

For simultaneous recordings of electrophysiologic and CBF changes, we focused our studies on the caudate-putamen (CPu) and whisker area of the barrel field (S1BF), and the thalamic ventral posterior medial nucleus (VPM), because these regions were, respectively, found to be maximally involved, by SWD on our fMRI study on these rats. We sampled electrophysiology and CBF from established (Nersesyan, Herman et al. 2004) as well as coordinates showing optimal responses to both whisker stimulation and SWD (in S1BF) and then used these for group analyses in the remaining all animals. Total SWD recorded for electrophysiology were of 213, 456, and 243 from CPu, S1BF, and VPM, respectively, from 13 animals with an average duration of 5.45± 2.1 seconds (mean ± SD; range, 1.77–15.76 seconds). CBF data represented were from 180, 399, and 330 SWD from CPu, S1BF, and VPM, respectively, from 11 animals with an average duration of 4.81±2.58 seconds (mean ± SD; range, 1.38–16.91 seconds). A total of 104 whisker stimulation (32 from CPu, 41 from S1BF, and 31 from VPM) responses were recorded with constant stimulus duration of 4 seconds. In all rats, spontaneous SWD induced a noticeable CBF increase in S1BF and VPM and decreases in CPu. We already reported negligible CBF increases in V1M (Nersesyan, Herman et al. 2004). The CBF changes correlated strongly with multiunit neuronal activity, which showed a prominent increase in MUA power during SWDs in S1BF, VPM. These increases were associated with small increase in CPu. The onset of CBF increases in S1BF was delayed by approximately 1 or 2 seconds after the onset of SWD. After the seizure, CBF decreased to basal levels with a lag of approximately 2 seconds. The mean peak increases in MUA

power and CBF during SWD were much greater in S1BF than in VPM. S1BF and VPM shows 21.84% and 34.37% increase, respectively, in LFP signal whereas 12.75% and 14.57% increase in MUA in S1BF and VPM, respectively. S1BF and VPM show 5.31% and 4.54% increase, respectively, in CBF signal. CPu show small increase in MUA which was associated with 88.57 % increase in LFP. This increase in MUA was associated with 3.71% decrease in CBF in CPu. Decrease in CBF signal in CPu was significantly different compared to S1BF and VPM ($p = 0.008$ and 0.028, respectively, with Bonferroni correction for multiple comparisons). CBF signals were not significantly different between S1BF and VPM ($p = 1.0$).

Neuronal activity and CBF during whisker stimulations in WAG/Rij Rats

Similar transient increases in neuronal firing and CBF were observed in the barrel cortex (S1BF) during whisker stimulation. However, during whisker stimulation, the increases in MUA power and in CBF were greater than during SWD in the same location. Therefore, smaller relative increases in neuronal firing and CBF were observed in the barrel cortex during SWD than during whisker stimulation. We found that mean changes in CBF during SWD and whisker stimulation were 5.30% and 9.92%, respectively. S1BF and VPM show 21.85% and 34.37% increase in LFP signal, respectively, whereas CPu shows big increase of 88.57%. Increase in LFP in CPu was significantly higher compared to S1BF and VPM ($p = 0.000$ and 0.000, respectively, with Bonferroni correction for multiple comparisons). LFP signals were marginally high in VPM compared to S1BF. S1BF and VPM show 12.75% and 14.57% increase, respectively, in MUA signal whereas CPu shows small increase of 3.62%. MUA signal in CPu was

significantly low compared to S1BF and VPM (p = 0.033 and 0.01, respectively, with Bonferroni correction for multiple comparisons). MUA signals were insignificantly different between S1BF and VPM (p = 1.0).

Electroencephalography Recordings in C3H/Hej Mice

We found that SWD were very uncommon at age 5 through age 15 days, then gradually increased, and appeared to plateau after age 25 days (Fig. 4). We did not find significant differences in the peak power spectrum amplitude between all four groups (age 5-7 days, age 20-22 days, age 31-40 days, age 51-62 days) using ANOVA (F=1.00, p=.40). Independent T-test between age group 5-7 days and age 20-22 days also did not reveal a significant difference in peak power spectrum amplitudes (T=-.841, p=0.41).

To investigate the progression of EEG changes during development, we analyzed repeated EEG samples at different ages ranging from 5d through 62d. We found that the percentage of time in SWD and the number of SWD per hour were very low below age 15 d, but then progressively increased, and appeared to level off after age 26-30d. Percent time in SWD increased from a mean of 0.1% in immature animals (age 5-15d) to 4% in adulthood (ages 26-62d) (p=0.006, two-tailed t-test). Comparing all 8 groups (age 5-7, 10-15, 20-22, 23-25, 26-30, 31-40, 41-50, 51-62) shows the differences in variance of percent time in seizures to be significant (F=15.82, p<.001, ANOVA), with an inflection point using raw data and a 3rd degree polynomial regression of 33.33 days. Similarly, the mean SWD per hour increased from 3 per hour in immature mice (5-15d) to 45 per hour in mature mice (26-62d) (p=0.0001) (Fig. 5). Comparing all 8 groups (age 5-7, 10-15, 20-22, 23-25, 26-30, 31-40, 41-50, 51-62) shows the difference in variance of

SWD per hour to be significant (F=18.59, p<.001, ANOVA) with an infelction point using raw data and a 3rd degree polynomial regression of 13.08 days. Seizure duration also showed a progressive, though less dramatic increase during development, with a mean seizure duration of 1.75 s at 5-15d, and 3.40 s at 26-62d (p=0.03). Comparing all 8 groups (age 5-7, 10-15, 20-22, 23-25, 26-30, 31-40, 41-50, 51-62) shows the difference in variance of seizure duration to be significant (F=14.00, p<.001, ANOVA) with an infelction point using raw data and a 3rd degree polynomial regression of 31.25 days.

2.4. Discussion:

Spike-Wave Discharges in WAG/Rij Rats: Role of Cortex, Thalamus, and Caudate

Multi-modal imaging of WAG/Rij rats during SWD with simultaneous EEG recordings allows for examining the time course and amplitude of BOLD signal changes in the WAG/Rij somatosensory cortex (S1BF), VPM nucleus of the thalamus and the caudate putamen. While the somatosensory cortex and thalamus both exhibit BOLD signal increases during SWD, the caudate consistently showed BOLD signal decreases (Fig. 1). Measurement of CBV using a paramagnetic contrast agent shows that the blood volume changes generally match the changes in the BOLD signal (Fig. 2).

Electrophysiology experiments utilizing microelectrodes and LDF probes showed that while BOLD signal increases in S1BF and VPM were matched by increases in CBF, local field potentials (LFP) and neuronal firing rates, BOLD signal decreases in the Caudate correlated with CBF decreases, greater increases in LFP that SBF or VPM and a greatly attenuated increase MUA compared to S1BF or VPM. Previous studies in

WAG/Rij rats have shown intense neuronal firing during SWD occurring in the somatosensory cortex and thalamus, with the perioral somatosensory cortex likely serving as the initial generator of SWD activity, and a relative sparing of other brain regions like the primary visual cortex (Meeren, Pijn et al. 2002; Blumenfeld 2003; Nersesyan, Herman et al. 2004; Nersesyan, Hyder et al. 2004).

Our data shows a strong temporal association in the BOLD, CBF, LFP, and MUA from the barrel cortex (SIBF) or thalamus (VPM) in the same direction, while the Caudate BOLD signal shows a decrease which begins earlier. Also, the Caudate shows a relatively larger LFP increase with longer duration compared the either SIBF or VPM. During spike-wave events thalamic and cortical neurons within a thalamocortical sector become tightly interlocked, supporting the idea that mutually interconnected neurons at the thalamic and cortical level are necessary to create and oscillating network to maintain SWD (Avoli, Gloor et al. 1983).

Using the time matched EEG data acquired during fMRI experiments allows for binning BOLD signal images with regard to SWD onset time, taken at different time points, we are able to investigate the time course of the BOLD signal with greater temporal resolution (Fig. 3). Interestingly we find a consistent initial dip in CBF signal recordings from the barrel cortex (SIBF), which precedes an initial dip in the BOLD signal, while this phenomenon was not seen in the Thalamus or Caudate (Fig. 3). Intrinsic optical signal imaging studies in rat models of 4-aminopyridine induced seizures have shown a focal and reproducible drop in oxygenated hemoglobin at the seizure onset, with confirmation using oxygen-sensitive electrodes (Bahar, Suh et al. 2006).

The benefits of high magnetic field strength (9 Tesla) imaging include both greater temporal and spatial resolution enabling region of interest analysis. The advantages of a quantitative modeling of the hemodynamic response, by using experimental data and measurements of the BOLD (Fig. 1) and CBF responses, include a more specific assessment of brain physiology, including insight into neurovascular coupling and the shape of the neural response itself (Buxton, Uludag et al. 2004).

Caudate recordings of BOLD and CBF from our study show a consistent decrease during seizures, beginning at seizure onset and resolving to baseline at 6-7 seconds after seizure onset. Human functional imaging has show frequent task-independent decreases, suggesting there may be a baseline or resting state of the human brain (Raichle, MacLeod et al. 2001). This implies that the decrease in BOLD and CBF may be related to pathologically induced changes that may contribute to the deficits seen in absence seizures. Whether there is functional impairment of the caudate-putamen, and what the symptomatic effect would be from such impairment remains unkown.

C3H/Hej Mouse Epileptogenesis:

At the youngest ages, the few SWD that occurred had a somewhat irregular morphology, and the spikes tended to have a relatively broad appearance. As the animals matured, SWD morphology became more regular in rhythm, and the spikes appeared more narrow (Fig. 4). The shape, and different phases of the spikes and slow waves in C3H/HeJ mice were similar to those reported in other rodent models (Sitnikova and van Luijtelaar 2007), with a large negative-going spike, and a relatively small negative slow wave in each cycle. Seizure morphology also changed during development in the

C3H/Hej mouse, with older animals exhibiting SWD that had a higher frequency, more regular rhythm, and narrower spikes (Fig. 4). We observed the emergence and development of SWD in C3H/HeJ mice, with the most rapid changes occurring over a time period from approximately 15 to 25 days of age, apparent in the number of SWD per hour (Fig. 5). We define a SWD as a pattern of rhythmic activity on electroencephalography with both a spike and a wave component with a frequency of 6-8 hz lasting at least 1 second. The total percent time in SWD also was very low before day 15 and subsequently increased rapidly, but the plateau after day 26 was not as apparent, possibly because SWD duration showed a trend towards continued slight increases after day 26 (Fig. 5).

Based on our findings we propose that SWD development in this model can be described in three stages. In the "immature stage," up to age 15 days, SWD-like events, possibly larval SWD or a related developmental phenomenon, were observed on average only 3 times per hour. These events may indicate an early predisposition to later development of fully realized SWD in C3H/Hej mice, or may represent other related rhythmic brain activity. SWD-like event morphology in the immature stage was characterized by irregular rhythm, relatively broad spikes, slow fundamental frequency (5-6 Hz), and brief duration (mean 1.75 s). In the "transitional stage" from 16 through 25 days, SWD incidence, duration, and fundamental frequency gradually increased. In the "mature stage," after approximately day 26 (or perhaps somewhat later with regard to SWD duration) SWD were observed an average of 45 times per hour. Mature SWD had a more regular rhythm, narrower spikes, higher fundamental frequency (7-8 Hz), and longer duration (mean 3.4 s).

While EEG recordings from implanted skull electrodes allowed for good characterization of SWD events in young and adult mice, more refined electrophysiology techniques would better localize regional brain involvement during SWD in this mouse model. One limitation of our study then is the lack of microelectrode recordings from specific cortical and subcortical brain areas during SWD. Future investigations will focus on refining the spatial characterization of SWD in C3H/Hej mice through more invasive electrophysiology techniques. In addition, we assumed that the SWD were bilaterally symmetrical, and we recorded from only one side, however further studies with bilateral recordings may be beneficial. Furthermore, the evolution of epileptogenesis in this model may be better characterized through improved analysis methods such as averaged time-frequency wavelet analysis at different ages.

While no previous studies have analyzed the development of epilepsy in the C3H/HeJ mouse in detail, extensive characterization has been completed in two other rodent models of absence epilepsy, rats of the WAG/Rij strain (Coenen and Van Luijtelaar 1987; Coenen and Van Luijtelaar 2003) and GAERS (Vergnes, Marescaux et al. 1982; Vergnes, Marescaux et al. 1986; Marescaux and Vergnes 1995; Danober, Deransart et al. 1998). Researchers have previously concluded that the seizures in these strains of rats are morphologically, behaviorally, and pharmacologically similar to the absence seizures experienced by human patients (Micheletti, Vergnes et al. 1985; Van Luijtelaar and Coenen 1988; Coenen, Drinkenburg et al. 1992; Marescaux, Vergnes et al. 1992; Marescaux and Vergnes 1995; van Luijtelaar, Drinkenburg et al. 2002; Coenen and Van Luijtelaar 2003).

WAG/Rij rats exhibit almost no spike-wave activity at age 75 d, approximately 5 – 7 SWD per hour at 140 d, and 16 – 18 SWD per hour at 245 d (Coenen and Van Luijtelaar 1987). The cumulative duration of the spike-wave complexes increases in parallel, from close to zero at 75 d, to approximately 25 and 75 seconds per hour at the ages of 140 days and 245 days, respectively (Coenen and Van Luijtelaar 1987). GAERS show essentially no SWD activity through 30 days of age, after which point SWD activity increases until the age of four months, when all tested GAERS show SWD activity, and SWD become even more severe at age six months (Vergnes, Marescaux et al. 1986; Marescaux, Vergnes et al. 1992; Marescaux and Vergnes 1995).

The C3H/HeJ mouse model for human absence epilepsy was described relatively recently (Frankel, Beyer et al. 2005) and is particularly promising for studying epileptogenesis because of the earlier age of SWD onset, and the known genetic defect in this model (Beyer, Deleuze et al. 2008). Like the rat models, epileptic activity in C3H/HeJ mice is morphologically, behaviorally, and pharmacologically similar to human absence epilepsy (Frankel, Beyer et al. 2005). Previous characterization of the C3H/HeJ model revealed SWD activity with burst frequencies of 7 – 8 Hz and epileptiform activity in mice as young as 3.5 weeks. We observed that the age of SWD development in C3H/HeJ mice was between age 15-25 d, which was substantially earlier than in either GAERS or WAG/Rij rats. We also observed that the morphology and power spectra of SWD in mature C3H/HeJ mice were similar to rat models (Drinkenburg, van Luijtelaar et al. 1993; Blumenfeld, Klein et al. 2008), but that at earlier ages, the power spectrum peaked at lower frequencies.

Backcross studies in C3H/HeJ mice have shown a recessive, non-Mendelian mode of inheritance of the absence epilepsy phenotype. It was recently found that the absence seizures in C3H/HeJ mice are due to a mutation of the AMPA receptor subunit *Gria4*, which is predominantly present in the thalamic reticular nucleus (Beyer, Deleuze et al. 2008). Gria4 mutants display enhanced synaptic excitation of inhibitory thalamic reticular neurons, with increased duration of synaptic responses. Seizure genesis in *Gria4* mutants may then occur because of stronger inhibition of thalamic relay cells and the promotion of rebound burst firing responses (Beyer, Deleuze et al. 2008). Enhanced firing of thalamic reticular neurons has previously been implicated in triggering the transition from normal activity to SWD generation (Blumenfeld and McCormick 2000).

Several possible maturational changes could affect the time course of seizure onset in this model of absence epilepsy. Differential production of hormones throughout the life of the organism has been shown to affect neural circuits and epileptic phenomena (Mattson and Cramer 1985; Morrell 1992), however, sexual maturity in mice occurs at about 7 weeks (Suckow, Brayton et al. 2001), substantially after the time of SWD onset. Developmental changes in the expression of voltage-gated ion channels have been reported previously in SWD models and could play a role (Klein, Khera et al. 2004; Strauss, Kole et al. 2004; Blumenfeld, Klein et al. 2008), as could changes in GABA receptor expression (Brooks-Kayal, Shumate et al. 2001). Another age-related change which occurs with appropriate timing to participate in the emergence of SWD in this model, is the switch of the GABA receptor's activity from excitatory to inhibitory, dependent on the chloride transporter (Plotkin, Snyder et al. 1997; Dzhala, Talos et al. 2005; Ben-Ari 2006; Huberfeld, Wittner et al. 2007; Munoz, Mendez et al. 2007; Kahle

and Staley 2008). While these are a few possible mechanisms for the development of SWD in the C3H/HeJ model as it ages, numerous other possibilities exist (Jensen and Baram 2000; Ben-Ari and Holmes 2006; Dube, Brewster et al. 2007; Scharfman 2007).

In conclusion, we observed the early appearance of SWD activity in C3H/HeJ mice, precursors of which are possibly seen on the fifth postnatal day. Between age 15 and 25 d there is a marked increase in the number of SWD per hour, and a progressive maturational development of SWD morphology, frequency, and duration. Future investigations of the C3H/HeJ model should include the assessment of early interventions in this model, to determine if early treatment can suppress epileptogenesis as was observed in rats (Blumenfeld, Klein et al. 2008). This model could then be used to determine the critical periods for intervention, the appropriate treatment window, and eventually further elucidate the molecular mechanisms of epileptogenesis. Therefore, the C3H/HeJ model provides substantial hope for future epilepsy research, including investigations of primary prevention.

2.5. Future Directions:

Simultaneous EEG-fMRI has contributed greatly to our understanding of hemodynamic responses that precede, accompany and follow epileptiform discharges, and to our understanding of hemodynamic and metabolic responses to neuronal activity. Additionally, the use of simultaneous EEG-fMRI will open many lines of investigation and will continuously refine our understanding of the temporal and spatial characteristics of neuronal activity. BOLD signal acquisition is only one of many promising MRI

modalities, and it will become increasingly feasible to fully investigate the neuroenergetic basis of activity changes in the brain using multimodal techniques. The integration of measurements of BOLD-fMRI, CBV, and CBF can be used to obtain estimates of the $CMRO_2$, thereby allowing a full investigation into neuronal energetics (Davis, Kwong et al. 1998; Hyder, Kida et al. 2002; Smith, Blumenfeld et al. 2002; Hyder and Blumenfeld 2004; Shulman and Rothman 2004; Stefanovic, Warnking et al. 2004; Maandag, Coman et al. 2007).

Knowledge of epileptogenesis, particularly greater insight into the neuronal networks and changes involved, using many of the above tools, would increase our understanding of the pathology of epilepsy, and may reveal novel treatment modalities aimed at preventing rather than treating epilepsy, and other neurological disorders. Substantial work remains to be done to further elucidate the molecular mechanisms of epileptogenesis, with the goal being total epilepsy prevention. Specifically, a detailed knowledge of the appropriate time course for interventions is needed to lay the groundwork for future studies

Crucial questions regarding the localization of changes during epileptiform events, and other neuronal processes, remain unanswered. Which region(s) are involved in seizure onset and propagation? How do different regions of the brain vary in their hemodynamic and metabolic response regarding temporal and amplitude characteristics from varying stimuli or processes? How do these hemodynamic and metabolic responses relate to electrical activity before, during and after neuronal events? Similarly, crucial questions are still unanswered regarding the development of epilepsy. What are the changes in neural structures and function that accompany epileptogenesis? How might

knowledge of epileptogenesis be used to disrupt the development of neuropathology? Answering these questions will contribute to our understanding of neuronal function, and to the development of targeted investigations, and treatments, for epilepsy and other neurological disorders.

2.6. **Conclusions**:

EEG-fMRI studies in animals can contribute to our understanding of epilepsy, sensory-motor processing and other neuronal events, and the relationship between fMRI signals and neuronal activity. Regarding SWD localization, caudate recordings of BOLD and CBF from our study show a consistent decrease during seizures, that begins at seizure onset and resolves to baseline at 6-7 seconds after seizure onset, and a consistent initial dip in CBF signal recordings from the barrel cortex (SIBF) which precedes an initial dip in the BOLD signal, while this phenomenon was not seen in the Thalamus or Caudate. Electrophysiolgy data shows that this decrease corresponds to a relatively larger LFP increase with longer duration compared the either SIBF or VPM. We also characterize the development of epilepsy in the C3H/Hej mouse, a new model of absence epilepsy, showing the time course of seizure development.

Acknowledgements:

Thank you to Hal Blumenfeld, a great mentor and friend, whose integrity has taught me so much for science, and for life. Thank you also to Dario Englot, Asht Mishra and Michael Purcaro for their incredible help and patience. This work was supported by NIH R01 NS049307, P30 NS052519, and by the Loughridge family. Damien Ellens was supported by the Howard Hughes Medical Institute as a Medical Fellow.

Figure Legends:

Figure 1.

Example of BOLD fMRI changes during SWD in WAG/Rij rat at 9.4T

Simultaneous EEG-fMRI was used to select BOLD images acquired 2-4 seconds after SWD onset, these were then compared to baseline images acquired before SWD onset. The somatosensory cortex (S1BF) and thalamus (Thal) show prominent increases. The basal ganglia (Cpu) shows decreases. There is no change during SWD in the visual cortex (V1M) or hippocampus (Hc). Results are displayed as % change in fMRI signal (ΔS/S). Calculated from 26 image pairs. From (Mishra, Ellens et al. 2008).

Figure 2.

CBV changes during SWD in WAG/Rij rat at 9.4 T.

CBV calculated using measured CBV-weighted BOLD changes during SWD and measured resting transverse (T2) relaxation rates with and without contrast agent. Simultaneous EEG-fMRI was used to select CBV images acquired 2-4 seconds after SWD onset, these were then compared to baseline images acquired before SWD onset. From (Mishra, Ellens et al. 2008).

Figure 3.

High temporal resolution time course of fMRI % changes (ΔS/S) during SWD.

Mean fMRI time courses were obtained in ROIs for bilateral somatosensory cortex (S1BF), thalamus (Thal), and basal ganglia (Cpu) in 33 experiememtns (800+ individual

SWD events). Peak changes are approximately 3 seconds after SWD onset. fMRI data were aligned temporally to SWD onset, based on simultaneous EEG recordings, enabling data binning at 0.5 to 1.0 second resolution (results shows are from 1.0 second bins). Data first pooled within each experiment and then combined across experiments (n=33). From (Mishra, Ellens et al. 2008).

Figure 4.

Examples of EEG recordings showing SWD in C3H/HeJ mice at different ages. Frequency of SWD is less at age 23 d (A) than at age 59 d (B). The morphology of SWDs changed as the mice aged, with examples shown on more expanded time scale at age 5 d (C), 23 d (D), and 59 d (E). As mice increased in age, the spike-wave morphology became more regular, spikes became narrower, and SWD frequency increased. SWD shown in (D) and (E) are from intervals marked by horizontal lines in (A) and (B). The corresponding lower time resolution trace for (C) is not shown. EEG was recorded in a bipolar montage (frontal minus parietal) with negative voltages displayed as upgoing. From (Ellens, Hong et al. 2009).

Figure 5.

Quantification of seizure development in C3H/HeJ mice.

SWD were seen infrequently in 5-15 day old animals. SWD progressively increased and the frequency stabilized at 26 days old. (A) Percent time spent in SWD (=100 x time in SWD/total recording time). (B) Number of SWD per hour. (C) SWD duration. Number of C3H/HeJ mice recorded at each time point: 5-7d (n=9), 10-15d (n=6), 20-22d (n=8),

23-25d (n=5), 26-30d (n=7), 31-40d (n=11), 41-50d (n=5), and 51-62d (n=9). Values are mean ± SEM. From (Ellens, Hong et al. 2009).

Figures:

Figure 1.

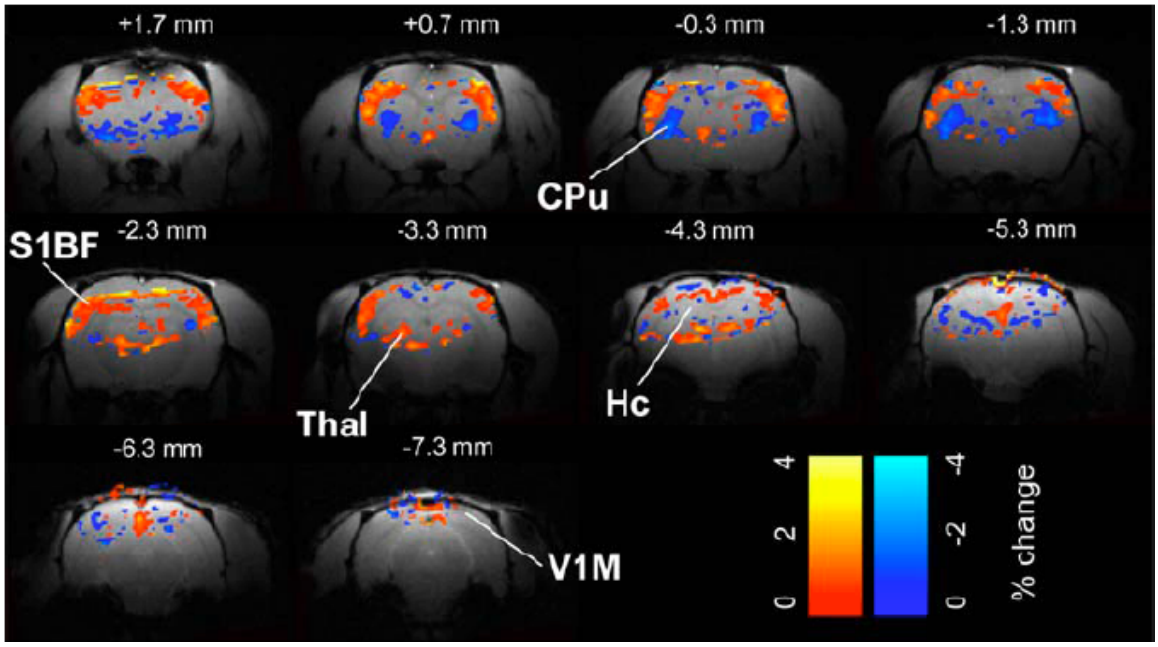

Figure 2.

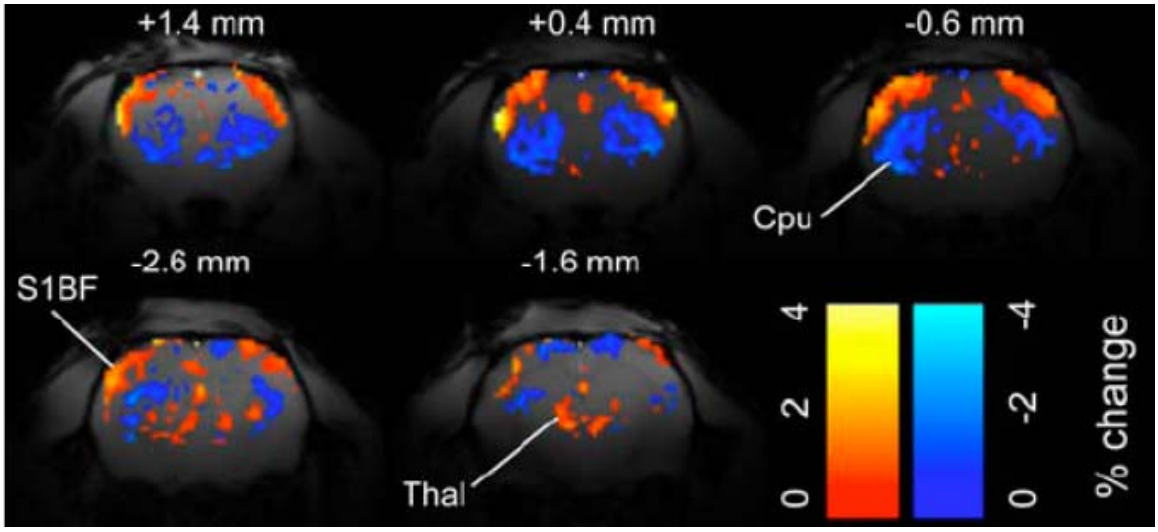

Figure 3.

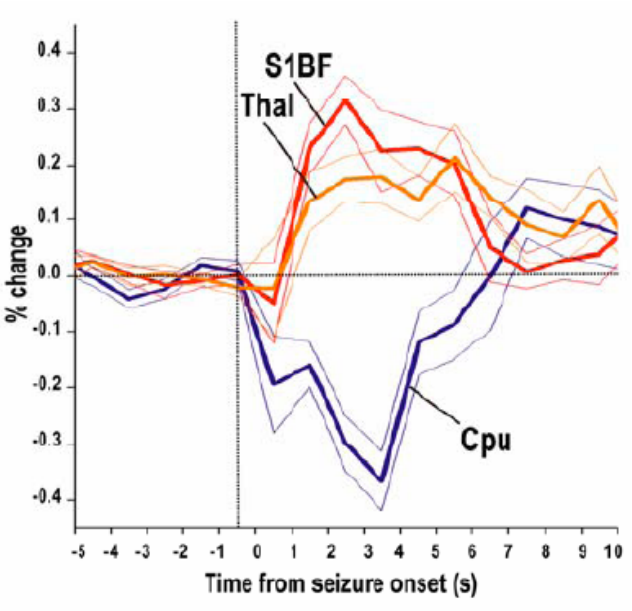

Figure 4.

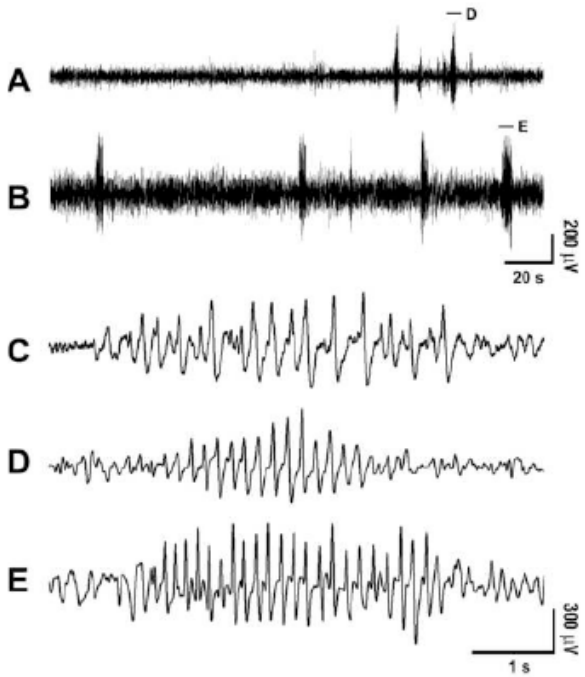

Figure 5.

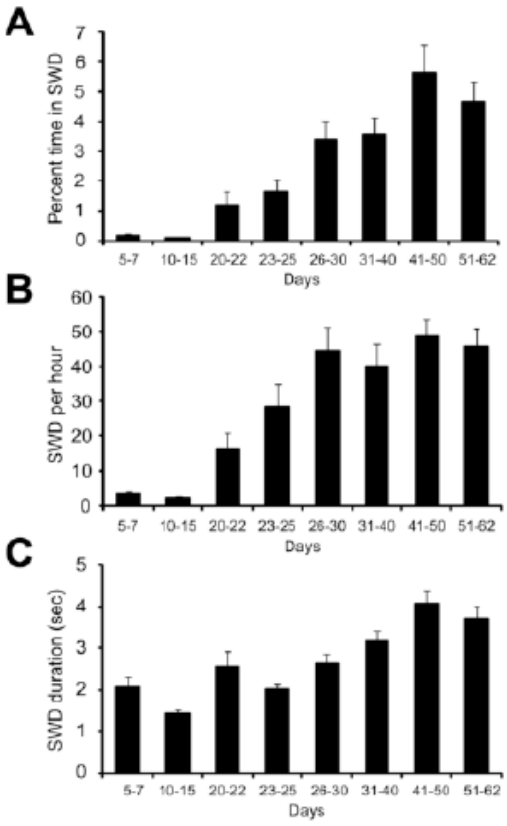
A
Percent time in SWD
0
1
2
3
4
5
6
7
5-7
10-15
20-22
23-25
26-30
31-40
41-50
51-62
Days
B
SWD per hour
0
10
20
30
40
50
60
5-7
10-15
20-22
23-25
26-30
31-40
41-50
51-62
Days
C
SWD duration (sec)
0
1
2
3
4
5
5-7
10-15
20-22
23-25
26-30
31-40
41-50
51-62
Days

References:

Aghakhani, Y., A. P. Bagshaw, et al. (2004). "fMRI activation during spike and wave discharges in idiopathic generalized epilepsy." Brain **127**(Pt 5): 1127-44.

Aghakhani, Y., E. Kobayashi, et al. (2006). "Cortical and thalamic fMRI responses in partial epilepsy with focal and bilateral synchronous spikes." Clin Neurophysiol **117**(1): 177-91.

Angenstein, F., E. Kammerer, et al. (2007). "Frequency-dependent activation pattern in the rat hippocampus, a simultaneous electrophysiological and fMRI study." NeuroImage **38**(1): 150-163.

Archer, J. S., D. F. Abbott, et al. (2003). "fMRI "deactivation" of the posterior cingulate during generalized spike and wave." Neuroimage **20**(4): 1915-22.

Austin, V. C., A. M. Blamire, et al. (2005). "Confounding effects of anesthesia on functional activation in rodent brain: a study of halothane and alpha-chloralose anesthesia." Neuroimage **24**(1): 92-100.

Avoli, M., P. Gloor, et al. (1983). "An analysis of penicillin-induced generalized spike and wave discharge using simultaneous recordings of cortical and thalamic single neurons." J Neurophysiol **50**: 819-837.

Avoli, M., P. Gloor, et al., Eds. (1990). Generalized Epilepsy. Boston, Birkhauser.

Babb, T. L. and W. Kupfer (1984). "Phagocytic and metabolic reactions to chronically implanted metal brain electrodes." Exp Neurol **86**(2): 171-82.

Bahar, S., M. Suh, et al. (2006). "Intrinsic optical signal imaging of neocortical seizures: the 'epileptic dip'." Neuroreport **17**(5): 499-503.

Behar, K. L., O. A. Petroff, et al. (1986). "Detection of metabolites in rabbit brain by 13C NMR spectroscopy following administration of [1-13C]glucose." Magnetic Resonance in Medicine **3**(6): 911-20.

Ben-Ari, Y. (2006). "Basic developmental rules and their implications for epilepsy in the immature brain." Epileptic Disord **8**(2): 91-102.

Ben-Ari, Y. and G. L. Holmes (2006). "Effects of seizures on developmental processes in the immature brain." Lancet Neurology **5**(12): 1055-63.

Ben-Ari, Y., J. Lagowska, et al. (1979). "A new model of focal status epilepticus: intra-amygdaloid application of kainic acid elicits repetitive secondarily generalized convulsive seizures." Brain Research **163**(1): 176-9.

Berger, H. (1929). "Ueber das Elektrenkephalogramm des Menschen." Arch f Psychiat **87**: 527.

Beyer, B., C. Deleuze, et al. (2008). "Absence seizures in C3H/HeJ and knockout mice caused by mutation of the AMPA receptor subunit Gria4." HMG Advance Access.

Blumenfeld, H. (2003). "From molecules to networks: cortical/subcortical interactions in the pathophysiology of idiopathic generalized epilepsy." Epilepsia **44 Suppl 2**: 7-15.

Blumenfeld, H. (2005). "Cellular and network mechanisms of spike-wave seizures." Epilepsia **46 Suppl 9**: 21-33.

Blumenfeld, H. (2005). "Consciousness and epilepsy: why are patients with absence seizures absent?" Prog Brain Res **150**: 271-86.

Blumenfeld, H. (2007). "Functional MRI studies of animal models in epilepsy." Epilepsia **48(Suppl. 4)**: 18-26.

Blumenfeld, H., J. P. Klein, et al. (2008). "Early treatment suppresses the development of spike-wave epilepsy in a rat model." Epilepsia **49 (3)**: 400–409.

Blumenfeld, H. and D. A. McCormick (2000). "Corticothalamic inputs control the pattern of activity generated in thalamocortical networks." Journal of Neuroscience **20**(13): 5153-62.

Blumenfeld, H., K. A. McNally, et al. (2004). "Positive and negative network correlations in temporal lobe epilepsy." Cerebral Cortex **14**(8): 892-902.

Blumenfeld, H., M. Rivera, et al. (2004). "Ictal neocortical slowing in temporal lobe epilepsy." Neurology **63**: 1015-1021.

Blumenfeld , H. and J. Taylor (2003). "Why do seizures cause loss of consciousness?" The Neuroscientist **9**(5): 301-310.

Brevard, M. E., P. Kulkarni, et al. (2006). "Imaging the neural substrates involved in the genesis of pentylenetetrazol-induced seizures." Epilepsia **47**(4): 745-54.

Brooks-Kayal, A. R., M. D. Shumate, et al. (2001). "gamma-Aminobutyric acid(A) receptor subunit expression predicts functional changes in hippocampal dentate granule cells during postnatal development." Journal of Neurochemistry **77**(5): 1266-78.

Busch, E., M. Hoehn-Berlage, et al. (1995). "Simultaneous recording of EEG, DC potential and diffusion-weighted NMR imaging during potassium induced cortical spreading depression in rats." NMR Biomed **8**(2): 59-64.

Buxton, R. B., K. Uludag, et al. (2004). "Modeling the hemodynamic response to brain activation." Neuroimage **23 Suppl 1**: S220-33.

Coenen, A. M., W. H. Drinkenburg, et al. (1992). "Genetic models of absence epilepsy, with emphasis on the WAG/Rij strain of rats." Epilepsy Research **12**(2): 75-86.

Coenen, A. M. and E. L. Van Luijtelaar (1987). "The WAG/Rij rat model for absence epilepsy: age and sex factors." Epilepsy Research **1**(5): 297-301.

Coenen, A. M. and E. L. Van Luijtelaar (2003). "Genetic Animal Models for Absence Epilepsy: A Review of the WAG/Rij Strain of Rats." Behav Genet **33**: 635-655.

Cox, G. A., C. M. Lutz, et al. (1997). "Sodium/hydrogen exchanger gene defect in slow-wave epilepsy mutant mice.[erratum appears in Cell 1997 Dec 12;91(6):861]." Cell **91**(1): 139-48.

Danneman, P. J. and T. D. Mandrell (1997). "Evaluation of five agents/methods for anesthesia of neonatal rats." Lab Anim Sci **47**(4): 386-95.

Danober, L., C. Deransart, et al. (1998). "Pathophysiological mechanisms of genetic absence epilepsy in the rat." Prog Neurobiol **55**: 27-57.

Davis, T. L., K. K. Kwong, et al. (1998). "Calibrated functional MRI: mapping the dynamics of oxidative metabolism." Proceedings of the National Academy of Sciences of the United States of America **95**(4): 1834-9.

Detre, J. A., J. S. Leigh, et al. (1992). "Perfusion imaging." Magnetic Resonance in Medicine **23**(1): 37-45.

Detre, J. A. and J. Wang (2002). "Technical aspects and utility of fMRI using BOLD and ASL." Clinical Neurophysiology **113**(5): 621-34.

Drinkenburg, W. H., E. L. van Luijtelaar, et al. (1993). "Aberrant transients in the EEG of epileptic rats: a spectral analytical approach." Physiol Behav **54**(4): 779-83.

Dube, C. M., A. L. Brewster, et al. (2007). "Fever, febrile seizures and epilepsy." Trends in Neurosciences **30**(10): 490-6.

Dzhala, V. I., D. M. Talos, et al. (2005). "NKCC1 transporter facilitates seizures in the developing brain.[see comment]." Nature Medicine **11**(11): 1205-13.

Ellens, D., E. Hong, et al. (2009). "Development of Spike-Wave Seizures in C3H/Hej Mice." Epilepsy Research **In Press**.

Englot, D. J., A. M. Mishra, et al. (2008). "Simultaneous fMRI and electrophysiology during intracerebral stimulation of partial seizures in rats." ISMRM Abs.

Fletcher, C. F., C. M. Lutz, et al. (1996). "Absence epilepsy in tottering mutant mice is associated with calcium channel defects." Cell **87**(4): 607-17.

Frankel, W. N., B. Beyer, et al. (2005). "Development of a new genetic model for absence epilepsy: spike-wave seizures in C3H/He and backcross mice." J Neurosci **25**(13): 3452-8.

Gibbs, F. A., W. G. Lennox, et al. (1934). "Cerebral blood flow preceding and accompanying epileptic seizures in man." Arch Neruol Psychiatry **32**: 257-272.

Gloor, P. (1985). "Neuronal generators and the problem of localization in electroencephalography: application of volume conductor theory to electroencephalography." J Clin Neurophysiol **2**(4): 327-54.

Gotman, J., C. Grova, et al. (2005). "Generalized epileptic discharges show thalamocortical activation and suspension of the default state of the brain." Proceedings of the National Academy of Sciences of the United States of America **102**(42): 15236-40.

Grohn, O. and A. Pitkanen (2007). "Magnetic resonance imaging in animal models of epilepsy-noninvasive detection of structural alterations." Epilepsia **48 Suppl 4**: 3-10.

Gruetter, R., E. J. Novotny, et al. (1994). "Localized 13C NMR spectroscopy in the human brain of amino acid labeling from D-[1-13C]glucose." J Neurochem **63**(4): 1377-85.

Gruetter, R., E. R. Seaquist, et al. (1998). "Localized in vivo 13C-NMR of glutamate metabolism in the human brain: initial results at 4 tesla." Developmental Neuroscience **20**(4-5): 380-8.

Guillemain, I., O. David, et al. (2007). "EEG and fMRI evidence for a cortical focus of absence seizures in the genetic absence rats from strasbourg (gaers)."

Hamandi, K., A. Salek-Haddadi, et al. (2006). "EEG-fMRI of idiopathic and secondarily generalized epilepsies." Neuroimage **31**(4): 1700-10.

He, J., I. M. Devonshire, et al. (2007). "Simultaneous laser Doppler flowmetry and arterial spin labeling MRI for measurement of functional perfusion changes in the cortex." Neuroimage **34**(4): 1391-404.

Hiremath, G. K. and I. M. Najm (2007). "Magnetic resonance spectroscopy in animal models of epilepsy." Epilepsia **48 Suppl 4**: 47-55.

Horsley, V. (1892). "An address on the origin and seat of epileptic disturbance." British Medical Journal **1**: 693-696.

Huberfeld, G., L. Wittner, et al. (2007). "Perturbed chloride homeostasis and GABAergic signaling in human temporal lobe epilepsy." J Neurosci **27**(37): 9866-73.

Hudetz, A. G. (2002). "Effect of volatile anesthetics on interhemispheric EEG cross-approximate entropy in the rat." Brain Res **954**(1): 123-31.

Hyder, F. (2004). "Neuroimaging with calibrated FMRI." Stroke **35**(11 Suppl 1): 2635-41.

Hyder, F. and H. Blumenfeld (2004). Relationship between CMRO2 and neuronal activity. Brain Energetics and Neuronal Activity: Applications to fMRI and Medicine. R. G. Shulman and D. L. Rothman. New York, John Wiley & Sons, Inc.**:** 173-194.

Hyder, F., I. Kida, et al. (2001). "Quantitative functional imaging of the brain: towards mapping neuronal activity by BOLD fMRI." NMR in Biomedicine **14**(7-8): 413-31.

Hyder, F., I. Kida, et al. (2002). Quantitative fMRI of rat brain by multi-modal MRI and MRS measurements. International Symposium on Brain Activation and CBF Control, International Congress Series.

Hyder, F., D. L. Rothman, et al. (2002). "Total neuroenergetics support localized brain activity: implications for the interpretation of fMRI.[comment]." Proceedings of the National Academy of Sciences of the United States of America **99**(16): 10771-6.

Ives, J. R., S. Warach, et al. (1993). "Monitoring the patient's EEG during echo planar MRI." Clin. Neurol. **87**: 417-420.

Jensen, F. E. and T. Z. Baram (2000). "Developmental seizures induced by common early-life insults: short- and long-term effects on seizure susceptibility." Mental Retardation & Developmental Disabilities Research Reviews **6**(4): 253-7.

Jones, M., J. Berwick, et al. (2005). "The effect of hypercapnia on the neural and hemodynamic responses to somatosensory stimulation." NeuroImage **27**(3): 609-623.

Jupp, B., J. P. Williams, et al. (2006). "MRI compatible electrodes for the induction of amygdala kindling in rats." Journal of Neuroscience Methods **155**(1): 72-76.

Kahle, K. T. and K. Staley (2008). "Altered neuronal chloride homeostasis and excitatory GABAergic signaling in human temporal lobe epilepsy." Epilepsy Curr **8**(2): 51-3.

Katariina M. Lahti, C. F. F. F. L. C. H. S. J. A. K. (1999). "Comparison of evoked cortical activity in conscious and propofol-anesthetized rats using functional MRI." Magnetic Resonance in Medicine **41**(2): 412-416.

Kayser, C., M. Kim, et al. (2004). "A comparison of hemodynamic and neural responses in cat visual cortex using complex stimuli." Cereb Cortex **14**(8): 881-91.

Kennan, R. P., J. Zhong, et al. (1994). "Intravascular susceptibility contrast mechanisms in tissue." Magn Reson Med **31**: 9-21.

Keogh, B. P., D. Cordes, et al. (2005). "BOLD-fMRI of PTZ-induced seizures in rats." Epilepsy Research **66**(1-3): 75-90.

Khubchandani, M., N. R. Jagannathan, et al. (2005). "Functional MRI shows activation of the medial preoptic area during sleep." Neuroimage **26**(1): 29-35.

Khubchandani, M., H. N. Mallick, et al. (2003). "Stereotaxic assembly and procedures for simultaneous electrophysiological and MRI study of conscious rat." Magnetic Resonance in Medicine **49**: 962-967.

Kida, I., R. P. Kennan, et al. (2000). "High-resolution CMR(O2) mapping in rat cortex: a multiparametric approach to calibration of BOLD image contrast at 7 Tesla." Journal of Cerebral Blood Flow & Metabolism **20**(5): 847-60.

Kida, I., D. L. Rothman, et al. (2007). "Dynamics of changes in blood flow, volume, and oxygenation: implications for dynamic functional magnetic resonance imaging calibration." Journal of Cerebral Blood Flow & Metabolism **27**(4): 690-6.

Klein, J. P., D. S. Khera, et al. (2004). "Dysregulation of sodium channel expression in cortical neurons in a rodent model of absence epilepsy." Brain Research **1000**: 102-109.

Krakow, K., P. J. Allen, et al. (2000). "EEG recording during fMRI experiments: image quality." Hum Brain Mapp **10**(1): 10-5.

Labate, A., R. S. Briellmann, et al. (2005). "Typical childhood absence seizures are associated with thalamic activation." Epileptic Disorders **7**(4): 373-7.

Laufs, H., U. Lengler, et al. (2006). "Linking generalized spike-and-wave discharges and resting state brain activity by using EEG/fMRI in a patient with absence seizures." Epilepsia **47**(2): 444-8.

Letts, V. A., R. Felix, et al. (1998). "The mouse stargazer gene encodes a neuronal Ca2+-channel gamma subunit.[see comment]." Nature Genetics **19**(4): 340-7.

Logothetis, N. K., J. Pauls, et al. (2001). "Neurophysiological investigation of the basis of the fMRI signal." Nature **412**(6843): 150-7.

Maandag, N. J., D. Coman, et al. (2007). "Energetics of neuronal signaling and fMRI activity." Proc Natl Acad Sci U S A **104**(51): 20546-51.

Makiranta, M., J. Ruohonen, et al. (2005). "BOLD signal increase preceeds EEG spike activity--a dynamic penicillin induced focal epilepsy in deep anesthesia." Neuroimage **27**(4): 715-24.

Makiranta, M. J., J. P. Jauhiainen, et al. (2002). "Functional magnetic resonance imaging of swine brain during change in thiopental anesthesia into EEG burst-suppression level--a preliminary study." Magma **15**(1-3): 27-35.

Mandeville, J. B., J. J. Marota, et al. (1999). "MRI measurement of the temporal evolution of relative CMRO(2) during rat forepaw stimulation." Magn Reson Med **42**(5): 944-51.

Marescaux, C. and M. Vergnes (1995). "Genetic Absence Epilepsy in Rats from Strasbourg (GAERS)." Ital J Neurol Sci **16**(1-2): 113-8.

Marescaux, C., M. Vergnes, et al. (1992). "Genetic absence epilepsy in rats from Strasbourg--a review." Journal of Neural Transmission. Supplementum **35**: 37-69.

Martin, C., M. Jones, et al. (2006). "Haemodynamic and neural responses to hypercapnia in the awake rat." European Journal of Neuroscience **24**(9): 2601-10.

Mason, G. F., K. L. Behar, et al. (1992). "NMR determination of intracerebral glucose concentration and transport kinetics in rat brain." Journal of Cerebral Blood Flow & Metabolism **12**(3): 448-55.

Mason, G. F., R. Gruetter, et al. (1995). "Simultaneous determination of the rates of the TCA cycle, glucose utilization, alpha-ketoglutarate/glutamate exchange, and glutamine synthesis in human brain by NMR." Journal of Cerebral Blood Flow & Metabolism **15**(1): 12-25.

Matsumoto, H. and C. A. Marsan (1964). "Cortical cellular phenomena in experimental epilepsy: Ictal manifestations." Experimental Neurology **9**: 305-326.

Mattson, R. H. and J. A. Cramer (1985). "Epilepsy, sex hormones, and antiepileptic drugs." Epilepsia **26 Suppl 1**: S40-51.

Meeren, H. K., J. P. Pijn, et al. (2002). "Cortical focus drives widespread corticothalamic networks during spontaneous absence seizures in rats." Journal of Neuroscience **22**(4): 1480-95.

Menon, R. S., S. Ogawa, et al. (1993). "Tesla gradient recalled echo characteristics of photic stimulation-induced signal changes in the human primary visual cortex." Magn Reson Med **30**(3): 380-6.

Micheletti, G., M. Vergnes, et al. (1985). "Antiepileptic drug evaluation in a new animal model: spontaneous petit mal epilepsy in the rat." Arzneimittel-Forschung **35**(2): 483-5.

Midzianovskaia, I. S., G. D. Kuznetsova, et al. (2001). "Electrophysiological and pharmacological characteristics of two types of spike-wave discharges in WAG/Rij rats." Brain Res **911**: 62-70.

Mirsattari, S. M., F. Bihari, et al. (2005). "Physiological monitoring of small animals during magnetic resonance imaging." Journal of Neuroscience Methods **144**(2): 207-13.

Mirsattari, S. M., J. R. Ives, et al. (2005). "Real-time display of artifact-free electroencephalography during functional magnetic resonance imaging and magnetic resonance spectroscopy in an animal model of epilepsy." Magnetic Resonance in Medicine **53**(2): 456-64.

Mirsattari, S. M., J. R. Ives, et al. (2007). "EEG monitoring during functional MRI in animal models." Epilepsia **48 Suppl 4**: 37-46.

Mirsattari, S. M., Z. Wang, et al. (2006). "Linear aspects of transformation from interictal epileptic discharges to BOLD fMRI signals in an animal model of occipital epilepsy." Neuroimage **30**(4): 1133-48.

Mishra, A., D. Ellens, et al. (2008). "Spatio-temporal dynamics of the BOLD fMRI signal changes and physiology during spike-wave seizures in WAG/Rij rats " Society for Neuroscience Abstract.

Mishra, A. M., U. Schridde, et al. (2007). "Physiology and imaging of increases and decreases in BOLD signals during spike-wave seizures in WAG/Rij rats." Online at http://web.sfn.org/.

Morrell, M. J. (1992). "Hormones and epilepsy through the lifetime." Epilepsia **33 Suppl 4**: S49-61.

Munoz, A., P. Mendez, et al. (2007). "Cation-chloride cotransporters and GABA-ergic innervation in the human epileptic hippocampus." Epilepsia **48**(4): 663-73.

Nakahata, K., H. Kinoshita, et al. (2003). "Mild hypercapnia induces vasodilation via adenosine triphosphate-sensitive K+ channels in parenchymal microvessels of the rat cerebral cortex." Anesthesiology **99**(6): 1333-9.

Negishi, M., M. Abildgaard, et al. (2004). "Removal of time-varying gradient artifacts from EEG data acquired during continuous fMRI." Clinical Neurophysiology **115**(9): 2181-92.

Nersesyan, H., P. Herman, et al. (2004). "Relative changes in cerebral blood flow and neuronal activity in local microdomains during generalized seizures." J Cereb Blood Flow Metab **24**(9): 1057-68.

Nersesyan, H., P. Herman, et al. (2004). "Relative changes in cerebral blood flow and neuronal activity in local microdomains during generalized seizures." J Cereb Blood Flow Metab **24**(9): 1057-1068.

Nersesyan, H., F. Hyder, et al. (2004). "Dynamic fMRI and EEG recordings during spike-wave seizures and generalized tonic-clonic seizures in WAG/Rij rats." J Cereb Blood Flow Metab **24**(6): 589-599.

Ogawa, S. and T. Lee (1992). "Blood oxygen level dependent MRI of the brain: effects of seizure induced by kainic acid in the rat." Proc Soc Magn Reson Med **1**: 501.

Ogawa, S., T. M. Lee, et al. (1990). "Brain magnetic resonance imaging with contrast dependent on blood oxygenation." Proceedings of the National Academy of Sciences of the United States of America **87**(24): 9868-72.

Ogawa, S., T. M. Lee, et al. (2000). "An approach to probe some neural systems interaction by functional MRI at neural time scale down to milliseconds." Proc Natl Acad Sci U S A **97**(20): 11026-31.

Ogawa, S., R. S. Menon, et al. (1998). "On the characteristics of functional magnetic resonance imaging of the brain." Annu Rev Biophys Biomol Struct **27**: 447-74.

Ogawa, S., R. S. Menon, et al. (1993). "Functional Brain mapping by blood oxygenation level-dependent contrast magnetic resonance imaging." Biophys J **64**: 803-812.

Opdam, H. I., P. Federico, et al. (2002). "A sheep model for the study of focal epilepsy with concurrent intracranial EEG and functional MRI." Epilepsia **43**(8): 779-87.

Paxinos, G. and C. Watson (1998). The rat brain in stereotaxic coordinates. San Diego, Academic Press.

Peeters, B. W. M. M., W. P. J. M. Spooren, et al. (1988). "The WAG/Rij rat model for absence epilepsy: Anticonvulsant drug evaluation." Neuroscience Research Communications **2**(2): 93-97.

Peeters, R. R., I. Tindemans, et al. (2001). "Comparing BOLD fMRI signal changes in the awake and anesthetized rat during electrical forepaw stimulation." Magn Reson Imaging **19**(6): 821-6.

Penfield, W. (1933). "The evidence for a cerebral vascular mechanism in epilepsy." Ann Int Med **7**: 303-310.

Phifer, C. B. and L. M. Terry (1986). "Use of hypothermia for general anesthesia in preweanling rodents." Physiol Behav **38**(6): 887-90.

Pinault, D., N. Leresche, et al. (1998). "Intracellular recordings in thalamic neurones during spontaneous spike and wave discharges in rats with absence epilepsy." J Physiol **509 (Pt 2)**: 449-56.

Plotkin, M. D., E. Y. Snyder, et al. (1997). "Expression of the Na-K-2Cl cotransporter is developmentally regulated in postnatal rat brains: a possible mechanism underlying GABA's excitatory role in immature brain." Journal of Neurobiology **33**(6): 781-95.

Raichle, M. E., A. M. MacLeod, et al. (2001). "A default mode of brain function." Proc Natl Acad Sci U S A **98**(2): 676-82.

Ritter, P. and A. Villringer (2006). "Simultaneous EEG-fMRI." Neuroscience & Biobehavioral Reviews **30**(6): 823-838.

Rothman, D. L., N. R. Sibson, et al. (1999). "In vivo nuclear magnetic resonance spectroscopy studies of the relationship between the glutamate-glutamine neurotransmitter cycle and functional neuroenergetics." Philosophical

Transactions of the Royal Society of London - Series B: Biological Sciences **354**(1387): 1165-77.

Sachdev, R. N., G. C. Champney, et al. (2003). "Experimental model for functional magnetic resonance imaging of somatic sensory cortex in the unanesthetized rat." Neuroimage **19**(3): 742-50.

Salek-Haddadi, A., L. Lemieux, et al. (2003). "Functional magnetic resonance imaging of human absence seizures." Annals of Neurology **53**(5): 663-7.

Salek-Haddadi, A., M. Merschhemke, et al. (2002). "Simultaneous EEG-Correlated Ictal fMRI." Neuroimage **16**(1): 32-40.

Scharfman, H. E. (2007). "The neurobiology of epilepsy." Current Neurology & Neuroscience Reports **7**(4): 348-54.

Schridde, U., M. Khubchandani, et al. (2007). "Negative BOLD with large increases in neuronal activity." Cerebral Cortex, In Press.

Schwartz, T. H. and T. Bonhoeffer (2001). "In vivo optical mapping of epileptic foci and surround inhibition in ferret cerebral cortex." Nature Medicine **7**(9): 1063-7.

Shmuel, A., M. Augath, et al. (2006). "Negative functional MRI response correlates with decreases in neuronal activity in monkey visual area V1." Nature Neuroscience **9**(4): 569-77.

Shmuel, A., M. Augath, et al. (2006). "Negative functional MRI response correlates with decreases in neuronal activity in monkey visual area V1." Nat Neurosci **9**(4): 569-77.

Shulman, R. G., F. Hyder, et al. (2001). "Cerebral energetics and the glycogen shunt: neurochemical basis of functional imaging." Proceedings of the National Academy of Sciences of the United States of America **98**(11): 6417-22.

Shulman, R. G., F. Hyder, et al. (2002). "Biophysical basis of brain activity: implications for neuroimaging." Quarterly Reviews of Biophysics **35**(3): 287-325.

Shulman, R. G., D. L. Rothman, et al. (2004). "Energetic basis of brain activity: implications for neuroimaging." Trends in Neurosciences **27**(8): 489-95.

Shulman, R. G., D. L. Rothman, et al. (1999). "Stimulated changes in localized cerebral energy consumption under anesthesia." Proceedings of the National Academy of Sciences of the United States of America **96**(6): 3245-50.

Shulman, R. G. and D. L. E. Rothman (2004). Brain Energetics and Neuronal Activity: Applications to fMRI and Medicine. New York, John Wiley & Sons, Inc.

Shyu, B. C., C. Y. Lin, et al. (2004). "A method for direct thalamic stimulation in fMRI studies using a glass-coated carbon fiber electrode." J Neurosci Methods **137**(1): 123-31.

Sijbers, J., B. Vanrumste, et al. (2000). "Automatic localization of EEG electrode markers within 3D MR data." Magn Reson Imaging **18**(4): 485-8.

Sitnikova, E. and G. van Luijtelaar (2007). "Electroencephalographic characterization of spike-wave discharges in cortex and thalamus in WAG/Rij rats." Epilepsia **48**(12): 2296-311.

Sloan, T. B. (1998). "Anesthetic effects on electrophysiologic recordings." J Clin Neurophysiol **15**(3): 217-26.

Smith, A. J., H. Blumenfeld, et al. (2002). "Cerebral energetics and spiking frequency: The neurophysiological basis of fMRI." Proc Natl Acad Sci U S A **99**(16): 10765-10770.

Snead, O. C., 3rd, A. Depaulis, et al. (1999). "Absence epilepsy: advances in experimental animal models." Advances in Neurology **79**: 253-78.

Stefanovic, B., J. M. Warnking, et al. (2004). "Hemodynamic and metabolic responses to neuronal inhibition." Neuroimage **22**(2): 771-8.

Strauss, U., M. H. Kole, et al. (2004). "An impaired neocortical Ih is associated with enhanced excitability and absence epilepsy." European Journal of Neuroscience **19**(11): 3048-58.

Suckow, M. A., C. Brayton, et al. (2001). "The laboratory mouse." from http://www.neurosciencenetbase.com/ejournals/books/book_km.asp?id=970

Tallgren, P., S. Vanhatalo, et al. (2005). "Evaluation of commercially available electrodes and gels for recording of slow EEG potentials." Clin Neurophysiol **116**(4): 799-806.

Tenney, J. R., T. Q. Duong, et al. (2004). "FMRI of brain activation in a genetic rat model of absence seizures." Epilepsia **45**(6): 576-82.

Tenney, J. R., T. Q. Duong, et al. (2003). "Corticothalamlic modulation during absence seizures in rats: A functional MRI assessment." Epilepsia **44**(9): 1133-1140.

Tenney, J. R., P. C. Marshall, et al. (2004). "fMRI of generalized absence status epilepticus in conscious marmoset monkeys reveals corticothalamic activation." Epilepsia **45**(10): 1240-7.

Tolias, A. S., F. Sultan, et al. (2005). "Mapping cortical activity elicited with electrical microstimulation using FMRI in the macaque." Neuron **48**(6): 901-11.

Turner, R., P. Jezzard, et al. (1993). "Functional mapping of the human visual cortex at 4 and 1.5 tesla using deoxygenation contrast EPI." Magn Reson Med **29**(2): 277-9.

V.C. Austin, A. M. B. S. M. G. M. J. O. N. P. S. P. M. M. N. R. S. (2003). "Differences in the BOLD fMRI response to direct and indirect cortical stimulation in the rat." Magnetic Resonance in Medicine **49**(5): 838-847.

Van Audekerkea, J., R. Peeters, et al. (2000). "Special designed RF-antenna with integrated non-invasive carbon electrodes for simultaneous magnetic resonance imaging and electroencephalography acquisition at 7T." Magn Reson Imaging **18**(7): 887-91.

Van Camp, N., R. D'Hooge, et al. (2003). "Simultaneous electroencephalographic recording and functional magnetic resonance imaging during pentylenetetrazol-induced seizures in rat." Neuroimage **19**: 627-636.

van Luijtelaar, E. L. and A. M. Coenen (1986). "Two types of electrocortical paroxysms in an inbred strain of rats." Neurosci Lett **70**(3): 393-7.

Van Luijtelaar, E. L. and A. M. Coenen (1988). "Circadian rhythmicity in absence epilepsy in rats." Epilepsy Research **2**(5): 331-6.

van Luijtelaar, E. L., W. H. Drinkenburg, et al. (2002). "Rat models of genetic absence epilepsy: what do EEG spike-wave discharges tell us about drug effects?" Methods Find Exp Clin Pharmacol **24 Suppl D**: 65-70.

van Rijn, C. M., M. S. Sun, et al. (2004). "Effects of the combination of valproate and ethosuximide on spike wave discharges in WAG/Rij rats." Epilepsy Research **59**(2-3): 181-9.

Vergnes, M., C. Marescaux, et al. (1986). "Ontogeny of spontaneous petit mal-like seizures in Wistar rats." Brain Research **395**(1): 85-7.

Vergnes, M., C. Marescaux, et al. (1982). "Spontaneous paroxysmal electroclinical patterns in rat: a model of generalized non-convulsive epilepsy." Neurosci Lett **33**(1): 97-101.

Weisskoff, R. M., C. S. Zuo, et al. (1994). "Microscopic susceptibility variation and transverse relaxation: theory and experiment." Magn Reson Med **31**: 601-610.

Winters, W. D. (1976). "Effects of drugs on the electrical activity of the brain: anesthetics." Annu Rev Pharmacol Toxicol **16**: 413-26.

Wood, A. K., A. M. Klide, et al. (2001). "Prolonged general anesthesia in MR studies of rats." Acad Radiol **8**(11): 1136-40.

Yang, Y., H. Wen, et al. (1999). "Comparison of 3D BOLD Functional MRI with Spiral Acquisition at 1.5 and 4.0 T." NeuroImage **9**(4): 446-451.

Young, G. B., J. R. Ives, et al. (2006). "A comparison of subdermal wire electrodes with collodion-applied disk electrodes in long-term EEG recordings in ICU." Clin Neurophysiol **117**(6): 1376-9.